The transgenerational effects of solar short-UV radiation differed in two accessions of Vicia faba L. from contrasting UV environments

Yan, Yan

2020-05

Yan , Y , Stoddard , F L , Neugart , S , Oravec , M , Urban , O , Sadras , V O & Aphalo , P J 2020 , ' The transgenerational effects of solar short-UV radiation differed in two accessions of Vicia faba L. from contrasting UV environments ' , Journal of Plant Physiology , vol. 248 , 153145 . https://doi.org/10.1016/j.jplph.2020.153145

http://hdl.handle.net/10138/343194
https://doi.org/10.1016/j.jplph.2020.153145

acceptedVersion

The transgenerational effects of solar short-UV radiation differed in two accessions of *Vicia faba* L. from contrasting UV environments

Yan Yan[1*], Frederick L. Stoddard[2], Susanne Neugart[3], Michal Oravec[4], Otmar Urban[4], Victor O. Sadras[5,6], Pedro J. Aphalo[1]

1. Viikki Plant Science Centre (ViPS), Department of Biosciences, 00014, University of Helsinki, Finland
2. Department of Agricultural Sciences, Viikki Plant Science Centre (ViPS) and Helsinki Sustainability Centre, 00014, University of Helsinki, Finland
3. Leibniz-Institute of Vegetable and Ornamental Crops, Großbeeren, Germany
4. Global Change Research Institute CAS, Brno, Czech Republic
5. South Australian Research and Development Institute, Adelaide, Australia
6. The University of Adelaide, School of Agriculture, Food and Wine, Australia

* For correspondence. E-mail: yan.z.yan@helsinki.fi. Phone: +358466534366. Address: Viikinkaari 1, Helsinki, Finland.

ABSTRACT

Background and Aims UVB radiation can rapidly induce gene regulation leading to cumulative changes for plant physiology and morphology. We hypothesized that a transgenerational effect of chronic exposure to solar short UV modulates the offspring's responses to UVB and blue light, and the transgenerational effect is genotype dependent. **Methods** We established a factorial experiment combining two *Vicia faba* L. accessions, two parental UV treatments (full sunlight and exclusion of short UV, 290-350 nm), and four offspring light treatments from the factorial combination of UVB and blue light. The accessions were Aurora from Southern Sweden, and ILB938 from Andean region of Colombia and Ecuador. **Key Results** The transgenerational effect influenced morphological responses to blue light differently in the two accessions. In Aurora, when UVB was absent, blue light increased shoot dry mass only in plants whose parents were protected from short UV. In ILB938, blue light increased leaf area and shoot dry mass more in plants whose parents were exposed to short UV than those that were not. Moreover, when the offspring was exposed to UVB, the transgenerational effect decreased in ILB938 and disappeared in Aurora. For flavonoids, the transgenerational effect was detected only in Aurora: parental exposure to short UV was associated with a greater induction of total quercetin in response to UVB. Transcript abundance was higher in Aurora than in ILB938 for both *CHALCONE SYNTHASE* (99-fold) and *DON-GLUCOSYLTRANSFERASE 1* (19-fold). **Conclusions** The results supported both hypotheses. Solar short UV had transgenerational effects on progeny responses to blue and UVB radiation, and they differed between the accessions. These transgenerational effects could be adaptive by acclimation of slow and cumulative morphological change, and by early build-up of UV protection through flavonoid accumulation on UVB exposure. The differences between the two accessions aligned with their adaptation to contrasting UV environments.

Key words Genotype-dependent, faba bean (*Vicia faba* L.), flavonoids, transgenerational effect, UVB radiation, blue light

INTRODUCTION

For plants, light is not only an energy source for photosynthesis but also a source of information that modulates growth and development (Aphalo and Ballare, 1995; Chen et al., 2004). Different wavebands of sunlight are perceived through different families of photoreceptors. Phytochromes mediate perception of red and far-red light (Smith, 2000), while cryptochromes (CRY), phototropins and members of the ZTL/FKF1/LKP2 family mediate perception of UVA and blue light (Lin, 2000; Pudasaini and Zoltowski, 2013). UVR8 (UV RESISTANCE LOCUS8) absorbs UVB and UVA and mediates UV acclimation in plants (Brown and Jenkins, 2008; Rizzini *et al.*, 2011; Rai *et al.*, 2019; Brelsford *et al.*, 2019).

Plant UVB responses have been assessed using so called “low” fluence rates (usually near but still above ambient levels in sunlight) or “high” fluence rates (well above ambient levels in sunlight) with treatments spanning from seconds to days (Brown and Jenkins, 2008; Christie *et al.*, 2012; Hideg *et al.*, 2013; Jansen *et al.*, 2019). Most of these studies have used an exaggerated UVB to photosynthetically active radiation (PAR) photon ratio. Chronic and acute exposure to UVB radiation have been shown to induce different responses through different underlying mechanisms (Ulm *et al.*, 2004).

Acute and high doses of UVB can directly damage DNA and indirectly affect programmed cell death as a result of massive production of reactive oxygen species (ROS) that overwhelms the plant’s antioxidant capacity (Hideg et al., 2013; Li et al., 2013). In contrast, chronic exposure to UVB radiation at ecologically relevant doses can trigger acclimation by inducing increased antioxidant capacity and optical shielding, for example through regulation of biosynthesis of phenylpropanoids or flavonoids (Hideg et al., 2013), inhibition of hypocotyl and stem

elongation, or development of thicker leaves (Jansen, 2002; Favory *et al.*, 2009; Wargent *et al.*, 2009; Jenkins, 2014). Apart from UVB, both blue and UVA radiation stimulate the accumulation of phenolic compounds (Fuglevand et al., 1996; Agati and Tattini, 2010) and lead to more compact plant growth (de Wit *et al.*, 2016). Blue and UV radiation trigger morphological changes that are partially mediated through changes in phytohormone metabolism and catabolism (Jansen, 2002; de Wit *et al.*, 2016). In addition, blue light is the most effective part of the spectrum in inducing stomatal opening (Zeiger, 1984; Dumont *et al.*, 2013), while the effect of UVB on this response is inconsistent (Musil and Wand, 1993; Ge *et al.*, 2014).

Flavonoid glycosides are phenolic compounds that predominantly accumulate in the vacuoles of epidermal and sub-epidermal cells and serve as sunscreen that protects inner mesophyll cells from harmful levels of UVB radiation (Harborne and Williams, 2000). Chalcone synthase (CHS) is the first enzyme in the biosynthetic pathway of flavonoids, thus controlling the commitment of phenolic precursors to synthesis of flavonoids versus phenolic acids. Blue and UVA radiation increase the transcript abundance of *CHS* through CRY1 (Wade et al., 2002), while UVB increases it through UVR8 (Favory *et al.*, 2009).

Evolutionarily, plant responses to light involve genetic differentiation from natural selection and phenotypic plasticity, which is the ability for one genotype to produce different phenotypes under various environments (Sultan, 2000). Transgenerational plasticity occurs when the environment experienced by the parents shapes the reaction norm of their offspring (Sultan, 1996; Thiede, 2006; Salinas *et al.*, 2013; Fenesi *et al.*, 2014). It relates to non-genetic inheritance, defined as "any effect on the offspring phenotype brought about by the transmission of factors other than DNA sequences from parents or more remote ancestors" (Bonduriansky and Day, 2009). Transgenerational effects vary among genotypes in a species

from different environments (Groot *et al.*, 2017; Lampei *et al.*, 2017) which implies that genetic variation from natural selection could play a role in transgenerational plasticity (Sultan, 2017). Parental light environment (light vs. shade) has been reported to affect the life cycle of the offspring in *Campanulastrum americanum* (L.) Small (Galloway and Etterson, 2007). Given the rapid nature of UVB sensing and regulation of UV responsive genes, Müller-Xing *et al*. (2014) have questioned the existence of transgenerational UV effects in plants, but empirical evidence is lacking. An even less investigated question is whether chronic exposure to solar UV radiation at ambient doses would have a transgenerational effect on the response to light of the offspring.

Plant response to UV has been investigated in crop species because of its potential effect on yield (Jia et al., 2009; Shinkle et al., 2010; Kravets et al., 2012; Martínez-Lüscher et al., 2013), but these studies have given little attention to transgenerational effects of UV. Faba bean (*Vicia faba* L.) is a legume crop domesticated at the western end of the Fertile Crescent that spread from there across Eurasia, Northern Africa and eventually the Americas (Lawes et al., 1983; Caracuta et al., 2015). At high elevation (around 3000 m) in the Andean region of Colombia and Ecuador, plants are exposed to strong UV radiation, whereas at the high latitude of southern Sweden, they receive relatively little UV radiation. Our previous study with two accessions of *Vicia faba* from these two regions showed differential responses to solar UV and blue light, including different flavonoid profile and gene expression patterns (Yan *et al.*, 2019).

This study tested two hypotheses: chronic exposure of the parental plant to solar short-UV affects the progeny response to blue and UVB radiation, and the response would differ in the two accessions of *Vicia faba* according to the UV environment where they have been adapted to.

MATERIALS AND METHODS

Overview

To test our hypotheses, we conducted a factorial experiment combining two faba bean accessions, two parental treatments, and four offspring light treatments (Fig. 1). The accessions were Aurora, adapted to high-latitude and low-altitude environments in Sweden, and ILB938, adapted to the low-latitude and high-altitude Andean region of Colombia and Ecuador. Two UV treatments (full sunlight and exclusion of short-UV, 290-350 nm) were applied to parental plants. Their progenies ($+UV_{parental}$ and $-UV_{parental}$) were grown in a controlled environment under four light treatments from the factorial combination of UVB and blue light.

Plant growth conditions and light treatments for parents

From a previous outdoor experiment (Yan *et al.*, 2019), *Vicia faba* accessions Aurora and ILB938 were grown under either a ">290 nm" filter (UV transparent) or a ">350 nm" filter (excluding short-UV, 290–350 nm) (Table 1A) outdoors from 4 May to 13 June 2016, and transferred to the greenhouse before flowering to complete seed production while avoiding cross-pollination. Parental treatments could affect embryo development (Rohde and Junttila, 2007; Kvaalen and Johnsen, 2008), thus, moving plants before flowering also excluded the possible direct treatment effect on the embryo. The average condition in the greenhouse was 21°C air temperature, 70% relative humidity, 300 μmol m^{-2} s^{-1} PAR, and the seeds were harvested on 20 August 2016. All plants were assumed to be self-pollinated as the greenhouse excluded pollinators. The progenies of plants grown under the ">290 nm" filter were termed $+UV_{parental}$, and those of plants grown under the ">350 nm" filter were termed $-UV_{parental}$ (Table 1A).

Plant growth conditions and light treatments for offspring

The seeds were imbibed overnight in tap water, inoculated with rhizobium (*R. leguminosarum* biovar *vicieae*, Elomestari OY, Tornio, Finland), and sown into 1-L pots containing pre-fertilized nursery peat (Kekkilä P6, Finland) and vermiculite (Vermipu, Finland) (2:1 by volume). Plants were watered regularly during the experiment.

The pots were arranged in a split-plot design, where the main plot was assigned to four light treatments (Table 1B) and the sub-plots were randomly allocated to the parental UV treatments and cultivars. The seeds were sown into pots under the light treatments. In the reach-in growth chambers (FitoClima D1200 PLLH, Aralab, Rio de Mouro, Portugal) the height of the rack was adjusted so that the top of the plants was 15 cm below the light. The positions of pots under each light treatment were rearranged twice a week to ensure a homogenous light environment for plants under the same treatment.

The growing conditions were 21°C and 70% relative humidity during the 14 h light phase and 16°C and 60% relative humidity during the 10 h dark phase. The CO_2 concentration was 400 µmol mol^{-1}. The PAR was set to simulate the natural light rhythm, gradually increasing from 70 µmol m^{-2} s^{-1} to 630 µmol m^{-2} s^{-1} during 4 h from 7:00 AM, maintained at 630 µmol m^{-2} s^{-1} for 6 h, and then gradually decreasing to 70 µmol m^{-2} s^{-1} over 4 h. The PAR was provided by LED lights (B50 spectra AP67, Valoya oy, Helsinki, Finland). Before plant emergence, four light treatments were established with the factorial use of a plastic sheet (Yellow acrylic, PLEXIGLAS 1C33 GT, Evonik, Germany) excluding blue light and special UVB-emitting 40W fluorescent tubes (QUV UVB-313 EL fluorescent lamp, Q-lab, Boston, UK) filtered as described below to give four light treatments at peak PAR: 1) UVB+Blue+; 2) UVB+Blue−; 3) UVB−Blue+; 4) UVB−Blue− (Table 1B, Supplemental Table S4). The output of LEDs was adjusted so that the PAR photon irradiance was the same for the four light treatments. For all four treatments, the UVB lamps were turned on for 6 h when PAR was at its maximum, while no UVB radiation was given for the rest of photoperiod. Since UVB lamps also emit moderate

amounts of UVA and small amounts of UVC, they were wrapped with cellulose diacetate film (0.095 mm thick, Kotelo-Rauma oy, Rauma, Finland) to exclude UVC radiation in treatments 1) and 2). Similarly, UVB lamps were wrapped with polyester film (0.125 mm thick, Autostat CT5, Thermoplast, Helsinki, Finland) to exclude both UVC and UVB in treatments 3) and 4). The light conditions in all treatments were measured with an array spectrometer (Maya200 Pro, Ocean Optics, Largo, USA) using a straylight-correction procedure (Ylianttila *et al.*, 2005). The experiment was replicated for four rounds, in which the positions of light treatments in the two chambers were rearranged. Each replicate round of the experiment lasted 28 days.

The estimated yearly maximum UVB irradiance is more than 50% higher in the Ecuadorian Andean region than in Southern Sweden, and solar UV radiation is much more effective in Ecuador than in Southern Sweden (effective irradiances of 0.75 W m^{-2} vs. 0.25 W m^{-2}, using GEN(G)) (Yan *et al.*, 2019). In the present experiment, the GEN(G) irradiance was 0.55 W m^{-2}. Thus, the UVB light condition was intermediate between the conditions at the place of origins of the two accessions.

Plant morphological and physiological measurements

Seed supplies and germination were unequal so the number of plants in each subplot varied. For each parental UV treatment of each accession, 1–5 plants under each light treatment (in 84% of cases, there were 2–3 plants) were used for morphological and physiological measurements (6–15 plants for four replicates; see Supplementary Data Table S1 for details of sample size). Stem length and dry mass, leaf number, leaf dimensions (length, width, area) and leaf dry mass were measured 28 d after sowing. Dry mass was measured in samples dried at 75°C for 4 d. Four to six leaves per plant were harvested and scanned for leaf area measurement with imageJ (Rasband, 2008). Specific leaf area (SLA) was calculated by dividing the area of these leaves by their dry mass, and specific stem length (SSL) was calculated dividing stem length by stem

dry mass. An equation was fitted to relate leaf area with leaflet width and length (see "Statistical analysis", below). For the un-scanned leaves (leaflet width and length measured), leaf area was calculated by using the fitted leaf area equation, and the corresponding leaf dry mass was calculated by dividing leaf area by SLA. Total leaf area per plant was estimated by multiplying average single leaf area with average leaf number per replicate.

Dry matter ratios can bias estimates of dry matter allocation where treatments affect plant size (Poorter and Sack, 2012), so the stem-to-shoot dry mass ratio ($M_{stem/shoot}$) and leaf-to-shoot dry mass ratio ($M_{leaf/shoot}$) were calculated.

The abaxial stomatal conductance was measured inside the growth chambers with an automatic transit-time porometer (AP4, Delta-T Devices, Cambridge, UK) 28 d after sowing, with two youngest fully expanded leaves measured per plant, and the average of the two were used for data analysis. The measurements started 2 h after PAR reached its maximum, and the doors were opened only briefly to keep the conditions inside the chambers undisturbed.

The indices for leaf epidermis flavonoid content (estimated by epidermal UVA absorbance 375 nm) and leaf chlorophyll index (estimated based on transmittance in the far-red and near-infrared) were assessed non-destructively with the Dualex Scientific^{+} device (Force-A ^{TM}, Paris, France) (Cerovic *et al.*, 2012) at the middle of the photoperiod 27 d after sowing. Leaves at three positions were used for measurements: the youngest fully expanded leaf, a middle leaf located at 50% height of the plant, and the bottom leaf.

Phenolic analysis by HPLC-DAD-ESI-MS^{n}

The youngest two fully expanded leaves were harvested from each plant (6–15 plants per light treatment per accession for four replicates), taken into liquid nitrogen and stored at -80°C until use. One leaf sample was used for phenolic compound and hormone analysis and the other for transcript abundance analysis. The samples were lyophilized in a freeze dryer (Savant

Modulyo® Freeze Dryer, Thermo Electron Corporation, USA) and ground to powder in a porcelain mortar. Flavonoids were analysed as previously described (Yan *et al.*, 2019).

ABA and JA quantification by HPLC-HRMS

The samples were homogenized using a mortar and pestle with the addition of liquid nitrogen, and hormones were extracted using a solution of methanol (VWR, Radnor, PE, USA), chloroform (Fisher Chemical, Waltham, MA, USA), and H_2O (1:2:2). A Purelab Classic system (ELGA LabWater, High Wycombe, Bucks, UK) was used to generate high purity water. An aliquot of the upper (polar) phase was used to analyze hormones (jasmonic acid and abscisic acid) in a high-performance liquid chromatography (HPLC) system UltiMate 3000 (Thermo Fisher Scientific, Waltham, MA, USA) coupled with a high-resolution mass spectrometer (HRMS) LTQ Orbitrap XL (Thermo Fisher Scientific, USA) and equipped with a HESI II (Heated electrospray ionization) source. A Hypersil Gold chromatographic column (150 mm x 2.1 mm, 3 µm; Thermo Fisher Scientific, USA) was used to separate metabolites, with a flow rate of mobile phases of 0.3 ml min^{-1} and a column temperature of 30°C, as described by Večeřová *et al.* (2016).

To identify the investigated hormones, a mass library, based on the in-house analyses of standards in MS and MSn modes, was used. Moreover, jasmonic acid (JA) and abscisic acid (ABA) were confirmed by retention time, m/z, Δppm, isotopic ratios, and dimers formed during the ionization. Jasmonic acid (m/z 211.13287, $\Delta ppm \leq 2$) and abscisic acid (m/z 265.14334, $\Delta ppm \leq 2$) were quantified in the more sensitive positive polarity mode. Calibration curves were used for quantification.

Gene expression analysis by quantitative real-time PCR (q-PCR)

We evaluated the transcript abundance of 8 key genes: *ELONGATED HYPOCOTYL 5* (*HY5*), involved in early stage of blue and UVB radiation signaling; *CHALCONE SYNTHASE* (*CHS*), *CHALCONE ISOMERASE* (*CHI*) and *DON-GLUCOSYLTRANSFERASE 1* (*DOGT1*), involved in the biosynthesis of flavonoid glycosides; *ABA INSENSITIVE 2* (*ABI2*), *AUXIN-INDUCIBLE 2-27* (*IAA5*) and *TYROSINE AMINOTRANSFERASE 3* (*TAT3*) which are responsive respectively to abscisic acid, auxin and jasmonic acid; and *HOMEOBOX-LEUCINE ZIPPER PROTEIN 4* (*ATHB4*), which is involved in the shade avoidance syndrome.

RNA extraction and cDNA synthesis were done as previously described (Yan *et al.*, 2019). The sequences of thirteen initially selected genes from *Arabidopsis thaliana* (L.) Heynh. obtained from The *Arabidopsis* Information Resource (TAIR) were used to BLAST the homologous genes in the *Medicago truncatula* Gaertn sequence database (LegumeIP, The Samuel Roberts Noble Foundation, Ardmore, OK, USA). The *Arabidopsis* and *M. truncatula* sequences were used to find the homologous genes in *Vicia faba* by BLASTing against a developing Trinity assembly of transcripts derived from RNAseq data of a mapping population (Frederick Stoddard, Jaakko Tanskanen, Alan Schulman, unpublished data). Primers for the 8 *Vicia faba* sequences were designed using Primer 3 (Untergasser et al., 2012), and the melting curve was validated for each pair of primers before using them in q-PCR. Supplementary Data Table S2 shows the primer sequence and gene information. The q-PCR experiment was conducted in a CFX384 Touch™ Real-Time PCR Detection System (Bio-Rad Laboratories, Inc., USA) using FIREPol® EvaGreen® q-PCR Mix Plus (Solis Biodyne, Tartu, Estonia). All samples from each replicate block were run on the same 384-well plate with 10 µl PCR reactions in triplicates. The cycle threshold values were determined using Bio-Rad CFX Manager and were imported into qbase ^{PLUS} 2.0 (Biogazelle, Belgium), where two reference genes (*ELF1A* and *CYP2*) (Gutierrez et al., 2011) (Supplementary Data Table S2) were used to normalize the q-PCR data. The reference genes had an average geNorm expression value M = 0.97 and coefficient of variation

CV = 0.4. After normalization, expression values were scaled to the average expression values of the specific run (Hellemans et al., 2007), $\log_{10}$-transformed and then exported from qbase^{PLUS} for statistical analyses in R-3.5.0 (R Core Team, 2018).

Statistical analysis

A linear mixed model with replicates (rounds) as random effects (LME) was fitted for all data analysis using the NLME package ('Linear Mixed-Effects Models: Basic Concepts and Examples', 2000) in R-3.5.0 (R Core Team, 2018). Factorial analysis of variance (ANOVA) was used to determine the significance of main effects (accessions, parental treatment, offspring light treatment) and their interactions. Where the ANOVA indicated interaction at $p < 0.1$ between two or more main effects, response differences were clarified by splitting data between, e.g., accessions and fitting models separately. For data with considerably different standard errors, five LME models were fitted: 1) the standard; 2) weighted for heterogeneity of variance dependent on plant size, "(weights = varPower(form = ~fitted(.))"; 3) weighted for heterogeneity of variance dependent on both plant size and light treatments, "(weights = varPower(form = ~fitted(.) | uv*blue))"; 4) weighted for different number of plants and plant size, "(weights = varPower(form = ~fitted(.) +sqrt(number of plants))"; 5) weighted for different number of plants, plant size and light treatments, "(weights = varPower(form = ~fitted(.) +sqrt(number of plants))". When one of the weightings improved the fit significantly according to Akaike's information criterion (AIC), that weighted model was chosen, otherwise the standard LME model with no weights was used. Models 4) and 5) never improved the fit. The profiles of flavonoid glycosides in the two accessions were assessed by principal component analysis (PCA) using R's prcomp() function. To ensure normal distribution, data used for PCA were $\log_2$ transformed molar concentrations (μmol g^{-1}). Figures were drawn using packages ggfortify and ggplot2 in R-3.5.0 (Tang *et al.*, 2016).

Linear models were fitted to describe leaf area as a function of the product of leaf width by leaf length (y = leaf area; x = $Width_{leaf}$ * $Length_{leaf}$; A = factor describing accessions; T = factor describing light treatments): "lm(y~A + x – 1)", "lm(y~A : x – 1)", "lm(y~ T + x – 1)" and "lm(y~ T : x – 1)". The best model "lm(y~A : x – 1)" was selected by using ANOVA and the equations were for Aurora, y= 0.720 * x and for ILB938, y= 0.725 * x.

RESULTS

Plant growth in response to parental and offspring light treatments

The effects of parental and offspring light treatments on eight traits of the two accessions are shown in Fig. 2, associated ANOVA in Supplementary Data Table S3 and separate ANOVA for the two accessions in Table 2. UVB radiation decreased stem length in both accessions, while the effect of blue light differed between accessions (Fig. 2A). In Aurora, blue light decreased stem length while, in ILB938, blue light increased stem length in $+UV_{parental}$ (p = 0.0004) but decreased it in $–UV_{parental}$ (p = 0.0004).

Aurora had greater leaf area than ILB938 (Fig. 2B). UVB decreased leaf area while blue light increased it. In ILB938, the absence of UVB heightened the increasing effect of blue light in $+UV_{parental}$ but not in $–UV_{parental}$. In $+UV_{parental}$, blue quadrupled leaf area when UVB was absent, while blue doubled it when UVB was present.

Aurora had greater shoot dry mass than ILB938 (Fig. 2C). In Aurora, UVB decreased shoot dry mass while the blue light effect depended on the presence of UVB and parental treatment, having no effect when UVB was absent in $–UV_{parental}$ but otherwise increasing shoot dry mass in the other three treatments. In ILB938, blue light increased shoot dry mass in $+UV_{parental}$ (p = 0.0006), and the size of effect depended on the presence of UVB, with blue tripling shoot dry mass when UVB was absent and doubling it when UVB was present.

The stem-to-shoot dry mass ratio ($M_{stem/shoot}$) was an unbiased estimate of dry matter allocation, as it was independent of shoot dry matter (Supplementary Data Figure S1). In Aurora, UVB reduced $M_{stem/shoot}$, while blue decreased the ratio more in + $UV_{parental}$ than in –$UV_{parental}$. In ILB938, blue light decreased $M_{stem/shoot}$ by 39% when UVB was absent but by only 13% when UVB was present. The response of leaf-to-shoot dry matter ratio ($M_{leaf/shoot}$) is complementary to that of $M_{stem/shoot}$ (Fig. 2E).

Aurora had thicker stems than ILB938, as indicated by its smaller specific stem length (SSL) (Fig. 2G). When UVB was absent, the blue light effect differed with parental treatment (p = 0.0004), especially in Aurora, where blue light increased stem thickness (decreased SSL by 7%) of –$UV_{parental}$ but did not affect that of +$UV_{parental}$. When UVB was present, blue light increased stem thickness (decreased SSL) in both accessions ($p < 0.0001$) regardless of parental UV-treatment.

Parental UV-treatments did not affect specific leaf area (SLA) (Fig. 2H). Blue light increased leaf thickness (decreased SLA) in both accessions ($p = 0.0001$) while the effect of UVB differed between accessions ($p = 0.020$), increasing leaf thickness (decreased SLA) of Aurora (p = 0.0011) but not affecting that of ILB938.

Stomatal conductance and leaf chlorophyll content

The UVB effect on stomatal conductance (g_s) differed between accessions (Fig. 2F). In Aurora, UVB decreased and blue light increased stomatal conductance, while in ILB938, the decreasing effect of UVB on stomatal conductance disappeared when blue light was present.

In Aurora the chlorophyll content per unit leaf area was higher in –$UV_{parental}$ than in +$UV_{parental}$ ($p < 0.0001$) but there was no difference in ILB938 due to treatment (Supplementary Data Figure S3).

Phenolics

In leaves at all positions of both accessions, the adaxial epidermis had 50% higher flavonoid concentration (estimated by epidermal UVA absorbance using Dualex) than the abaxial epidermis ($p < 0.0001$) (Supplementary Data Figure S2). In the youngest fully expanded leaf, both UVB ($p < 0.0001$) and blue ($p < 0.0001$) induced the accumulation of flavonoid in the adaxial epidermis in both accessions (Supplementary Data Figure S2 A), and the interaction between UVB and blue was significant in ILB938 ($p = 0.0083$) but not in Aurora ($p > 0.85$).

Twenty-four phenolic compounds (twelve kaempferol glycosides, nine quercetin glycosides and three phenolic acids) were identified and quantified by HPLC analysis of leaves sampled at the end of the experiment (Table 3).

Both mass and molar concentration of total kaempferol were higher in Aurora than in ILB938 ($p < 0.0001$), particularly for mass concentration (Fig. 3A & B). Twelve kaempferol glycosides were identified in Aurora and five in ILB938. Non-acetylated diglycosides, K[di], were more abundant in ILB938 (Fig. 4B) while acetylated monoglycosides, triglycosides and the tetraglycoside, K[ace.tri.tetra], were at higher concentrations in Aurora (Fig. 4A). Both UVB ($p = 0.0002$) and blue light ($p < 0.0001$) increased the concentrations of total kaempferols in the two accessions.

PCA for kaempferol glycosides highlighted the different profiles of kaempferol glycosides in the two accessions (Fig. 5). Parental UV treatment affected kaempferol profile in Aurora but not in ILB938, as shown in PC2 (Fig. 5A) and PC3 (Supplementary Data Figure S4). In PC2, the offspring light treatments were separated in ILB938, where K2-3 (Kaempferol-3-O-rhamnoglucoside), with the absolute weighting of 0.803, responded to blue and UVB (Fig. 4B, Fig. 5B). Table 4 shows the effect of parental and offspring light treatments and their interactions for each kaempferol group in both Aurora and ILB938; in Aurora, the total concentration of K[di] did not increase in response to UVB.

Blue light enhanced the inductive effect of UVB on the molar concentration of total quercetin in both accessions (Aurora: $p = 0.0003$; ILB938: $p < 0.0001$) (Fig. 3, Table 4). However, the effect of parental UV-treatment occurred only in Aurora: in response to UVB, the concentration of total quercetin increased less in $-UV_{parental}$ than in $+UV_{parental}$ ($p = 0.0005$), and the presence of blue light affected the size of the change. When blue was present, the fold changes in concentration by UVB were 3.5 in $-UV_{parental}$ compared to 6.2 in $+UV_{parental}$, while they were 3.6 vs. 4.8 when blue was absent (Fig. 3B).

Nine quercetin glycosides were identified in Aurora and only three in ILB938 (Fig. 6). Among the three in ILB938, Q3-4 triglycoside was minor, accounting for only 3.4% of the total (Fig. 6B). The PCA for quercetin glycosides separated the two accessions in PC1 (Fig. 7, Table 3). A transgenerational effect was detected for Aurora, as shown in PC2 (Fig. 7A) and PC3 (Supplementary Data Figure S5). The light treatments of Aurora were separated in PC1, while those of ILB938 were separated in PC2, with Q2-1 and Q2-2 (absolute weighting value of 0.644 and 0.655 respectively in PC2) showing the significant responses to light treatments (Fig. 7B, Table 3). Quercetin glycosides were grouped into Q[di] (diglycosides), mainly in ILB938, and Q[ace.tri] (acetylated monoglycosides and triglycosides), mainly in Aurora. The transgenerational effect of UV radiation on Aurora was detected for group Q[ace.tri] but not for group Q[di] (Table 4).

The total concentration of phenolic acids was higher in ILB938 than in Aurora ($p = 0.0004$), with no effect of parental or offspring light treatment (Fig. 8A). The phenolic acid composition was different in the two accessions: caffeoylmalic acid was detected in Aurora while coumaroylglucoside and feruloylglucoside were found in ILB938 (Fig. 8B).

Abscisic acid and jasmonic acid

The interaction between blue light and accession affected the molar concentration of ABA (p = 0.005) (Fig. 9A), but no effects of parental or offspring light treatments were detected in either accession. Similarly, no effect of parental or offspring light treatments was observed on JA concentration in either accession (Fig. 9B).

Transcript abundance

Transcript abundance varied between accessions for *CHS* (99-fold higher in Aurora) (p < 0.0001) and *DOGT1* (19-fold higher in Aurora) (p < 0.0001) (Fig. 10). Blue light increased the relative expression of three genes in Aurora: *HY5* by 4.4-fold (p = 0.0002), *CHI* by 3.1-fold (p = 0.0041) and *ABI2* by 6.1-fold (p < 0.0001) (Fig. 10). In ILB938, when UVB was present, the relative expression of *ATHB4* was 5.6-fold higher in $+UV_{parental}$ than in $-UV_{parental}$ (p = 0.031) (Fig. 10).

DISCUSSION

Agreeing with our hypothesis, multiple transgenerational effects of solar short-UV were detected in the morphology, flavonoids and gene expression of the two accessions, but not in stomatal conductance or phenolic acid concentrations.

Blue light stimulates stomatal opening (Zeiger, 1984; Dumont *et al.*, 2013), while UVB can either decrease (Nogues *et al.*, 1998; Ambasht and Agrawal, 1998; Ge *et al.*, 2014) or increase (Tevini *et al.*, 1983; Musil and Wand, 1993) it. The lack of transgenerational effect on stomatal conductance presumably results from the necessity for the plant to rapidly adjust stomatal aperture in response to its surroundings (Zeiger *et al.*, 1987). However, stomatal size and density could be altered when exposed to environmental factors in long term, such as by UV-B, drought and temperature (Gitz *et al.*, 2005; Sadras *et al.*, 2012). Aurora has higher stomatal conductance than ILB938 (Khan *et al.*, 2007; Yan *et al.*, 2019), but the accession-specific

response of stomatal conductance to UVB had not been investigated in *Vicia faba*. In the present study, UVB decreased stomatal conductance in Aurora regardless of blue light exposure, while UVB had no effect on stomatal conductance of ILB938 grown under blue light. This suggests that under sunlight where it is accompanied by blue light, UVB could be expected to affect steady-state stomatal conductance more in Aurora than in ILB938. However, this difference between accessions was smaller and not significant in a previous outdoor experiment (Yan *et al.*, 2019). This might be due to the big difference in UVB:UVA photon ratio between the two experiments: 0.014 in field experiment and 0.54 in the present one.

Despite the absence of a transgenerational effect, the concentration of total phenolic acids was higher in ILB938 than in Aurora. Since total flavonoid concentration and transcript abundance of *CHS* were both higher in Aurora than in ILB938, we speculate that phenolic acids might play a more important role in providing UV protection in ILB938, the high-altitude accession than in Aurora, the high-latitude one. Similarly, in *tt4* mutants of Arabidopsis with impaired flavonoid biosynthesis, the absence of leaf damage and the concurrent increase in phenolic acid concentration under UVB exposure indicated phenolic acid protection from UVB (Li *et al.*, 1993; Rai *et al.*, 2019).

UVB induces flavonoid accumulation in leaves (Hideg *et al.*, 2013), and blue light has been described as equally or more important under sunlight (Siipola *et al.*, 2015; Yan *et al.*, 2019). In our experiment, both blue and UVB induced the accumulation of epidermal and whole-leaf flavonoids, agreeing with previous studies in this species and others in growth chamber and outdoor conditions (Gonzalez *et al.*, 1998; Morales *et al.*, 2010, 2013; Siipola *et al.*, 2015; Yan *et al.*, 2019). In addition, our results show, for the first time, a strong positive interaction between blue and UVB, where the presence of blue potentiated the enhancement effect of UVB on total quercetin concentration. Compared with the previous outdoor experiment with the same two accessions of *Vicia faba* (Yan *et al.*, 2019), plants in the present experiment had similar

flavonoid profiles: nine of the 12 identified kaempferol glycosides were the same and four of the nine identified quercetin glycosides. In both experiments, the same two kaempferol glycosides (kaempferol-3-O-rhamnoarabinoside-7-O-rhamnoside and kaempferol-3-O-arabinoside-7-O-rhamnoside) were the most abundant in Aurora and ILB938, respectively, and the same quercetin glycoside (quercetin-3-O-rhamnoglucoside) was most abundant in ILB938. In addition, as in the outdoor experiment (Yan *et al.*, 2019), the kaempferol glycosides at higher concentration in Aurora had more sugar residues than those in ILB938.

The responses of gene expression also shared similar patterns with those from the outdoor experiment (Yan *et al.*, 2019). In Aurora, long-term exposure to blue light enhanced transcript abundance of some of the studied genes but UVB did not affect any of them, and the lack of transcriptional change in ILB938 suggested that it has lower sensitivity to long-term blue light. Moreover, as in the outdoor experiment (Yan *et al.*, 2019), *CHS* and *DOGT1* showed the greatest difference of transcript abundance between the two accessions, which in the case of *DOGT1* might help to explain the different glycosylation pattern of flavonoid glycosides in the two accessions. These similarities of flavonoid and gene expression patterns between the outdoor and controlled-environment studies with high PAR intensities suggest that the accessions had constitutive genetic differences in responses to light treatments. Furthermore, the transcriptional change induced by blue and the huge enhancement by UVB of the effect of blue light on quercetin concentration suggest that, under long-term light treatment, blue light could induce protection from subsequent acute UV exposure.

We found multiple accession-dependent transgenerational effects of solar short-UV on plant morphology, flavonoids and gene expression. Morphological responses to blue light were altered by the transgenerational effect of solar short-UV radiation. For Aurora, in response to deprivation of blue when UVB was absent, the parental UV treatment elicited a shade-avoidance syndrome including maintenance of growth and increased dry matter allocation to

stems at the expense of leaves in the progeny. For ILB938 in response to blue light, the transgenerational effect of UV increased plant growth without changing dry matter allocation. In contrast, dry mass in *Dimorphotheca sinuata* DC decreased when the two previous generations were exposed to enhanced UVB radiation in the greenhouse (Musil, 1996). When UVB was present, the transgenerational effects on morphological responses to blue light were smaller in ILB938 (stem length, shoot dry mass, total leaf area) and not detected in Aurora (shoot dry mass, SSL, $M_{stem/shoot}$, $M_{leaf/shoot}$). This indicates that transgenerational effects in part substituted for acclimation triggered by UV exposure in the current generation. Specific leaf area was decreased by UVB in Aurora but not in ILB938, while it was not affected by parental treatments in either accession. It can be concluded that transgenerational effects of solar short-UV on growth in response to blue light were mediated by different strategies in the two accessions from contrasting UV environments. Previous studies have described a tradeoff between acclimation to UV and shade in *Impatiens capensis* Meerb. due to competition for resources between stem elongation and phenolic synthesis (Dixon *et al.*, 2001; Weinig *et al.*, 2004).

In Aurora, the chlorophyll content per unit leaf area was lower in $+UV_{parental}$ than in $-UV_{parental}$, agreeing with earlier observations in *D. sinuata* (Musil, 1996). This transgenerational effect was absent in ILB938, the accession from a high UV environment.

The transgenerational effect of solar short-UV radiation was also detected for total quercetin concentration, kaempferol and quercetin derivative composition in Aurora: the parental exposure to solar short-UV resulted in a near-doubling of total quercetin derivative concentration in response to UVB (blue present) in the offspring. The lack of effect of parental UV treatments on flavonoids in ILB938 suggests that this accession either requires higher UV irradiation to trigger this response or is less sensitive to the lack of sustained UV memory from the previous generation. Furthermore, in ILB938, the transgenerational effect of solar short-UV

was found for the transcriptional abundance of *ATHB4*, which is a member of HD-Zip class-II transcription factors involved in shade avoidance syndrome and induced by low red/far-red ratio redundantly with other genes in this family (Sorin *et al.*, 2009). Since UV is involved in the interaction with the shade avoidance syndrome (Moriconi *et al.*, 2018), the higher expression of *ATHB4* in $+UV_{parental}$ under UVB suggests a possible transgenerational and complex interaction of UV and shade avoidance.

Transgenerational plasticity altering the phenotype of the offspring has been observed for many environmental cues. The progeny of drought-stressed parent plants of *Brassica napus* L. were more vigorous than those of unstressed parents (Hatzig *et al.*, 2018). Soil conditions experienced by the parent influenced size and seed germination of offspring in *Senecio vulgaris* L. (Aarssen and Burton, 1990). Parental light environments (understory vs. light gap) affected the life history (annual vs. biennial) in *Campanulastrum americanum* (Galloway and Etterson, 2007). Transgenerational effects associated with herbivory induced defensive resistance of progeny in *Raphanus raphanistrum* L. (Agrawal, 2002). Transgenerational plasticity was triggered for *Centella asiatica* (L.) Urban subjected to high/low light environments (Li *et al.*, 2018). These studies have shown that transgenerational plasticity could be adaptive, especially when progenies are exposed to environments similar to their parental environment. Nevertheless, in *D. sinuata,* the transgenerational effect of elevated UVB radiation on dry mass and chlorophyll concentration was attributed to damage (Musil, 1996). In the same species, increased leaf fluctuating asymmetry was interpreted as an indicator of DNA damage after four generations of successive exposure to enhanced UVB (Midgley *et al.*, 1998). These studies compared accumulated genetic damage across multiple generations under ambient sunlight (UVB_{BE} 2.5-8.9 kJ m^{-2} d^{-1}) and sunlight enhanced using UVB lamps (UVB_{BE} 4.7-11.4 kJ m^{-2} d^{-1}) as parental treatments. In contrast, we compared ambient sunlight to sunlight depleted of short-UV radiation using filters to assess whether the exposure to solar UV has a

transgenerational impact on plants, without presuming a negative effect. In spite of the difference in focus, results from our study and the study in *D. sinuata* agree in that differences in UV exposure in previous generations substantially affect the expression of morphological and physiological traits in the progeny. However, our interpretation is that the transgenerational effect of solar UV can lead to acclimation beneficial to the plants.

Transgenerational plasticity varied between genotypes from differently droughted environments in *Arabidopsis thaliana*, *Biscutella didyma* L. and *Bromus fasciculatus* C. Presl. (Groot *et al.*, 2017; Lampei *et al.*, 2017), and there was evidence of a clinal variation in the relative strength of transgenerational effects along an environmental gradient (Lampei *et al.*, 2017). Similarly, in our study, transgenerational plasticity to solar short-UV varied in the two accessions adapted to contrasting UV environments.

Transgenerational plasticity can be mediated through seed composition (Roach and Wulff, 1987; Mousseau and Fox, 1998; Bonduriansky and Day, 2009; Munday, 2014) or alteration of DNA methylation (Li *et al.*, 1993; Jablonka and Raz, 2009; Holeski *et al.*, 2012). In our study, seed size did not differ between parental UV treatments, so the transgenerational plasticity is likely to have been mediated through either seed nutrient storage in cotyledons or epigenetic mechanisms (Mousseau and Fox, 1998; Jablonka and Raz, 2009; Holeski *et al.*, 2012). Further studies are needed to identify the mechanisms of transgenerational effects of exposure to UV radiation and blue light and the possible differences between the two accessions of *Vicia faba*.

CONCLUSION

In conclusion, chronic exposure to solar short-UV had transgenerational effects on progeny morphology and flavonoids in response to blue and UVB. Although transcriptional responses to UV are rapid, the resulting changes in morphology are slow and cumulative, making it possible for transgenerational effects of solar short-UV to contribute to plant fitness through

morphological traits (c.f. Müller-Xing *et al.*, 2014). The accumulation of flavonoids can take place within hours, but their protection is needed immediately upon the start of UV exposure, so the transgenerational effect from solar short-UV can still play a role in UV protection. The two accessions in this study differed in their transgenerational response to solar short-UV, in line with their adaptation to contrasting UV environments.

SUPPLEMENTARY DATA

Supplementary data are available online and consist of the following. Figure S1: The figure shows stem-to-shoot dry mass ratio was unrelated to shoot dry mass. Figure S2: Absorbance of epidermal flavonoids per unit area on 27 d after sowing. Figure S3: Epidermal chlorophyll content per unit area on 27 d after sowing. Figure S4: Principal component analysis (PCA) of the kaempferol glycosides profile (PC1 v.s. PC3). Figure S5: Principal component analysis (PCA) of the quercetin glycosides profile (PC1 v.s. PC3). Table S1: Number of plants for four replicates per treatment per accession. Table S2: Genes chosen for q-PCR analysis and the corresponding primers. Table S3: P values from ANOVA for morphological and physiological traits.

ACKNOWLEDGEMENTS

This research was supported by China Scholarship Council. We thank Luis Morales for his suggestions for q-PCR. Analyses of plant hormones were supported by CZ.02.1.01/0.0/0.0/16_019/0000797 project (MEYS CR) and those of gene expression by the Academy of Finland grant 'Papugeno: Genomic tools for faba bean (*Vicia faba* L.) improvement for food and protein security' (decision 298314).

LITERATURE CITED

Aarssen LW, Burton SM. 1990. Maternal effects at four levels in *Senecio vulgaris* (Asteraceae) grown on a soil nutrient gradient. American Journal of Botany **77**, 1231–1240.

Agati G, Tattini M. 2010. Multiple functional roles of flavonoids in photoprotection. New Phytologist **186**, 786–793.

Agrawal AA. 2002. Herbivory and maternal effects: mechanisms and consequences of transgenerational induced plant resistance. Ecology **83**, 3408.

Ambasht NK, Agrawal M. 1998. Physiological and biochemical responses of *Sorghum vulgare* plants to supplemental ultraviolet-B radiation. Canadian Journal of Botany **76**, 1290–1294.

Aphalo PJ, Ballare CL. 1995. On the importance of information-acquiring systems in plant-plant interactions. Functional Ecology **9**, 5–14.

Bonduriansky R, Day T. 2009. Nongenetic inheritance and its evolutionary implications. Annual Review of Ecology, Evolution, and Systematics **40**, 103–125.

Brelsford CC, Morales LO, Nezval J, Kotilainen TK, Hartikainen SM, Aphalo PJ, Robson TM. 2019. Do UV-A radiation and blue light during growth prime leaves to cope with acute high light in photoreceptor mutants of *Arabidopsis thaliana* ? Physiologia Plantarum **165**, 537–554.

Brown BA, Jenkins GI. 2008. UV-B signaling pathways with different fluence-rate response profiles are distinguished in mature Arabidopsis leaf tissue by requirement for UVR8, HY5, and HYH. Plant physiology **146**, 576–88.

Caracuta V, Barzilai O, Khalaily H, Milevski I, Paz Y, Vardi J, Regev L, Boaretto E. 2015. The onset of faba bean farming in the Southern Levant. Scientific Reports **5**, 14370.

Cerovic ZG, Masdoumier G, Ghozlen N Ben, Latouche G. 2012. A new optical leaf-clip meter for simultaneous non-destructive assessment of leaf chlorophyll and epidermal

flavonoids. Physiologia Plantarum **146**, 251–260.

Chen M, Chory J, Fankhauser C. 2004. Light signal transduction in higher plants. Annual Review of Genetics **38**, 87–117.

Christie JM, Arvai AS, Baxter KJ, *et al.* 2012. Plant UVR8 photoreceptor senses UV-B by tryptophan-mediated disruption of cross-dimer salt bridges. Science **335**, 1492–1496.

Dixon P, Weinig C, Schmitt J. 2001. Susceptibility to UV damage in *Impatiens capensis* (Balsaminaceae): testing for opportunity costs to shade-avoidance and population differentiation. American Journal of Botany **88**, 1401–1408.

Dumont J, Spicher F, Montpied P, Dizengremel P, Jolivet Y, Le Thiec D. 2013. Effects of ozone on stomatal responses to environmental parameters (blue light, red light, CO2 and vapour pressure deficit) in three *Populus deltoides* × *Populus nigra* genotypes. Environmental Pollution **173**, 85–96.

Favory J-J, Stec A, Gruber H, *et al.* 2009. Interaction of COP1 and UVR8 regulates UV-B-induced photomorphogenesis and stress acclimation in Arabidopsis. The EMBO Journal **28**, 591–601.

Fenesi A, Dyer AR, Geréd J, Sándor D, Ruprecht E. 2014. Can transgenerational plasticity contribute to the invasion success of annual plant species? Oecologia **176**, 95–106.

Fuglevand G, Jackson JA, Jenkins GI. 1996. UV-B, UV-A, and blue light signal transduction pathways interact synergistically to regulate chalcone synthase gene expression in Arabidopsis. The Plant Cell **8**, 2347–57.

Galloway LF, Etterson JR. 2007. Transgenerational plasticity is adaptive in the wild. Science **318**, 1134–6.

Ge X-M, Zhu Y, He J-M. 2014. Cytosolic alkalisation and nitric oxide production in UVB-induced stomatal closure in Arabidopsis thaliana. Functional Plant Biology **41**, 803.

Gitz DC, Liu-Gitz L, Britz SJ, Sullivan JH. 2005. Ultraviolet-B effects on stomatal density,

water-use efficiency, and stable carbon isotope discrimination in four glasshouse-grown soybean (*Glyicine max*) cultivars. Environmental and Experimental Botany **53**, 343–355.

Gonzalez R, Wellburn AR, Paul ND. 1998. Dose responses of two pea lines to ultraviolet-B radiation (280-315 nm). Physiologia Plantarum **104**, 373–378.

Groot MP, Kubisch A, Ouborg NJ, Pagel J, Schmid KJ, Vergeer P, Lampei C. 2017. Transgenerational effects of mild heat in *Arabidopsis thaliana* show strong genotype specificity that is explained by climate at origin. New Phytologist **215**, 1221–1234.

Gutierrez N, Giménez MJ, Palomino C, Avila CM. 2011. Assessment of candidate reference genes for expression studies in *Vicia faba* L. by real-time quantitative PCR. Molecular Breeding **28**, 13–24.

Harborne JB, Williams CA. 2000. Advances in flavonoid research since 1992. Phytochemistry **55**, 481–504.

Hatzig S V., Nuppenau J-N, Snowdon RJ, Schießl S V. 2018. Drought stress has transgenerational effects on seeds and seedlings in winter oilseed rape (*Brassica napus* L.). BMC Plant Biology **18**, 297.

Hellemans J, Mortier G, De Paepe A, Speleman F, Vandesompele J. 2007. qBase relative quantification framework and software for management and automated analysis of real-time quantitative PCR data. Genome Biology **8**, R19.

Hideg É, Jansen MAK, Strid Å. 2013. UV-B exposure, ROS, and stress: inseparable companions or loosely linked associates? Trends in Plant Science **18**, 107–115.

Holeski LM, Jander G, Agrawal AA. 2012. Transgenerational defense induction and epigenetic inheritance in plants. Trends in Ecology & Evolution **27**, 618–626.

Jablonka E, Raz G. 2009. Transgenerational epigenetic inheritance: prevalence, mechanisms, and implications for the study of heredity and evolution. The Quarterly Review of Biology **84**, 131–76.

Jansen MAK. 2002. Ultraviolet-B radiation effects on plants: induction of morphogenic responses. Physiologia Plantarum **116**, 423–429.

Jansen MAK, Bilger W, Hideg É, *et al.* 2019. Editorial: Interactive effects of UV-B radiation in a complex environment. Plant Physiology and Biochemistry **134**, 1–8.

Jenkins GI. 2014. The UV-B photoreceptor UVR8: from structure to physiology. The Plant Cell **26**, 21–37.

Jia X, Ren L, Chen Q-J, Li R, Tang G. 2009. UV-B-responsive microRNAs in *Populus tremula*. Journal of Plant Physiology **166**, 2046–2057.

Khan HUR, Link W, Hocking TJ, Stoddard FL. 2007. Evaluation of physiological traits for improving drought tolerance in faba bean (*Vicia faba* L.). Plant and Soil **292**, 205–217.

Kvaalen H, Johnsen Ø. 2008. Timing of bud set in *Picea abies* is regulated by a memory of temperature during zygotic and somatic embryogenesis. New Phytologist **177**, 49–59.

Lampei C, Metz J, Tielbörger K. 2017. Clinal population divergence in an adaptive parental environmental effect that adjusts seed banking. New Phytologist **214**, 1230–1244.

Lawes D, Bond D, Poulsen M. 1983. Classification, origin, breeding methods and objectives. In. Hebblethwaite, PD (Ed.). The Faba Bean (*Vicia faba* L.): A Basis of Improvement. Butterworth, London, 24.

Li K, Chen J, Wei Q, Li Q, Lei N. 2018. Effects of Transgenerational Plasticity on Morphological and Physiological Properties of Stoloniferous Herb *Centella asiatica* Subjected to High/Low Light. Frontiers in Plant Science **9**, 1640.

Li J, Ou-Lee TM, Raba R, Amundson RG, Last RL. 1993. Arabidopsis flavonoid mutants are hypersensitive to UV-B irradiation. The Plant Cell **5**, 171–179.

Li J, Yang L, Jin D, Nezames CD, Terzaghi W, Deng XW. 2013. UV-B-induced photomorphogenesis in Arabidopsis. Protein & Cell **4**, 485–492.

Lin C. 2000. Plant blue-light receptors. Trends in Plant Science **5**, 337–342.

Linear Mixed-Effects Models: Basic Concepts and Examples. 2000. Mixed-effects models in S and S-PLUS. New York: Springer-Verlag, 3–56.

Martínez-Lüscher J, Morales F, Delrot S, Sánchez-Díaz M, Gomés E, Aguirreolea J, Pascual I. 2013. Short- and long-term physiological responses of grapevine leaves to UV-B radiation. Plant Science **213**, 114–122.

Midgley GF, Wand SJE, Musil CF. 1998. Repeated exposure to enhanced UV-B radiation in successive generations increases developmental instability (leaf fluctuating asymmetry) in a desert annual. Plant, Cell and Environment **21**, 437–442.

Morales LO, Brosche M, Vainonen J, Jenkins GI, Wargent JJ, Sipari N, Strid A, Lindfors A V, Tegelberg R, Aphalo PJ. 2013. Multiple roles for UV RESISTANCE LOCUS8 in regulating gene expression and metabolite accumulation in Arabidopsis under solar ultraviolet radiation. Plant Physiology **161**, 744–759.

Morales LO, Tegelberg R, Brosché M, Keinänen M, Lindfors A, Aphalo PJ. 2010. Effects of solar UV-A and UV-B radiation on gene expression and phenolic accumulation in *Betula pendula* leaves. Tree Physiology **30**, 923–934.

Moriconi V, Binkert M, Costigliolo C, Sellaro R, Ulm R, Casal JJ. 2018. Perception of sunflecks by the UV-B photoreceptor UV RESISTANCE LOCUS8. Plant Physiology **177**, 75–81.

Mousseau TA, Fox CW. 1998. The adaptive significance of maternal effects. Trends in Ecology & Evolution **13**, 403–407.

Müller-Xing R, Xing Q, Goodrich J. 2014. Footprints of the sun: memory of UV and light stress in plants. Frontiers in Plant Science **5**, 474.

Munday PL. 2014. Transgenerational acclimation of fishes to climate change and ocean acidification. F1000prime Reports **6**, 99.

Musil CF. 1996. Accumulated effect of elevated ultraviolet-b radiation over multiple

generations of the arid-environment annual *Dimorphotheca sinuata* DC. (Asteraceae). Plant, Cell and Environment **19**, 1017–1027.

Musil CF, Wand SJE. 1993. Responses of sclerophyllous ericaceae to enhanced levels of ultraviolet-B radiation. Environmental and Experimental Botany **33**, 233–242.

Nogues S, Allen DJ, Morison JIL, Baker NR. 1998. Ultraviolet-B radiation effects on water relations, leaf development, and photosynthesis in droughted pea plants. Plant Physiology **117**, 173–81.

Poorter H, Sack L. 2012. Pitfalls and Possibilities in the Analysis of Biomass Allocation Patterns in Plants. Frontiers in Plant Science **3**, 259.

Pudasaini A, Zoltowski BD. 2013. Zeitlupe senses blue-light fluence to mediate circadian timing in *Arabidopsis thaliana*. Biochemistry **52**, 7150–7158.

R Core Team. 2018. R: A Language and Environment for Statistical Computing.

Rai N, Neugart S, Yan Y, *et al.* 2019. How do cryptochromes and UVR8 interact in natural and simulated sunlight? Journal of Experimental Botany **70**, 4975–4990.

Rasband WS. 2008. Image J, version 1.41. Maryland, Bethesda: National Institutes of Health, URL: http://rsbweb. nih. gov/ij.

Rizzini L, Favory JJ, Cloix C, *et al.* 2011. Perception of UV-B by the Arabidopsis UVR8 protein. Science **332**, 103–106.

Roach DA, Wulff RD. 1987. Maternal effects in Plants. Annual Review of Ecology and Systematics **18**, 209–235.

Rohde A, Junttila O. 2007. Remembrances of an embryo: long-term effects on phenology traits in spruce. New Phytologist **177**, 2–5.

Sadras VO, Montoro A, Moran MA, Aphalo PJ. 2012. Elevated temperature altered the reaction norms of stomatal conductance in field-grown grapevine. Agricultural and Forest Meteorology **165**, 35–42.

Salinas S, Brown SC, Mangel M, Munch SB. 2013. Non-genetic inheritance and changing environments. Non-Genetic Inheritance **1**, 38–50.

Shinkle JR, Edwards MC, Koenig A, Shaltz A, Barnes PW. 2010. Photomorphogenic regulation of increases in UV-absorbing pigments in cucumber (*Cucumis sativus*) and *Arabidopsis thaliana* seedlings induced by different UV-B and UV-C wavebands. Physiologia Plantarum **138**, 113–121.

Siipola SM, Kotilainen T, Sipari N, Morales LO, Lindfors A V., Robson TM, Aphalo PJ. 2015. Epidermal UV-A absorbance and whole-leaf flavonoid composition in pea respond more to solar blue light than to solar UV radiation. Plant, Cell and Environment **38**, 941–952.

Smith H. 2000. Phytochromes and light signal perception by plants—an emergingsynthesis. Nature **407**, 585–591.

Sorin C, Salla-Martret M, Bou-Torrent J, Roig-Villanova I, Martínez-García JF. 2009. ATHB4, a regulator of shade avoidance, modulates hormone response in Arabidopsis seedlings. The Plant Journal **59**, 266–277.

Sultan SE. 1996. Phenotypic Plasticity for Offspring Traits in Polygonum Persicaria. Ecology **77**, 1791–1807.

Sultan SE. 2000. Phenotypic plasticity for plant development, function and life history. Trends in Plant Science **5**, 537–542.

Sultan SE. 2017. Developmental plasticity: re-conceiving the genotype. Interface Focus **7**, 20170009.

Tang Y, Horikoshi M, Li W. 2016. ggfortify: Unified Interface to Visualize Statistical Results of Popular R Packages. The R Journal **8**.

Tevini M, Iwanzik W, Teramura AH. 1983. Effects of UV-B radiation on plants during mild water stress II. Effects on Growth, Protein and Flavonoid Content. Zeitschrift für Pflanzenphysiologie **110**, 459–467.

Thiede DA. 2006. Maternal inheritance and its effect on adaptive evolution: a quantitative genetic analysis of maternal effects in a natural plant population. Evolution **52**, 998.

Ulm R, Baumann A, Oravecz A, Mate Z, Adam E, Oakeley EJ, Schafer E, Nagy F. 2004. Genome-wide analysis of gene expression reveals function of the bZIP transcription factor HY5 in the UV-B response of Arabidopsis. Proceedings of the National Academy of Sciences **101**, 1397–1402.

Untergasser A, Cutcutache I, Koressaar T, Ye J, Faircloth BC, Remm M, Rozen SG. 2012. Primer3—new capabilities and interfaces. Nucleic Acids Research **40**, e115–e115.

Večeřová K, Večeřa Z, Dočekal B, Oravec M, Pompeiano A, Tříska J, Urban O. 2016. Changes of primary and secondary metabolites in barley plants exposed to CdO nanoparticles. Environmental Pollution **218**, 207–218.

Wade HK, Bibikova TN, Valentine WJ, Jenkins GI. 2002. Interactions within a network of phytochrome, cryptochrome and UV-B phototransduction pathways regulate chalcone synthase gene expression in Arabidopsis leaf tissue. The Plant Journal **25**, 675–685.

Wargent JJ, Gegas VC, Jenkins GI, Doonan JH, Paul ND. 2009. UVR8 in *Arabidopsis thaliana* regulates multiple aspects of cellular differentiation during leaf development in response to ultraviolet B radiation. New Phytologist **183**, 315–326.

Weinig C, Gravuer KA, Kane NC, Schmitt J. 2004. Testing adaptive plasticity to UV: costs and benefits of stem elongation and light-induced phenolics. Evolution **58**, 2645.

de Wit M, Galvao VC, Fankhauser C. 2016. Light-mediated hormonal regulation of plant growth and development. Annual Review of Plant Biology **67**, 513–537.

Yan Y, Stoddard FL, Neugart S, Sadras VO, Lindfors A, Morales LO, Aphalo PJ. 2019. Responses of flavonoid profile and associated gene expression to solar blue and UV radiation in two accessions of *Vicia faba* L. from contrasting UV environments. Photochemical & Photobiological Sciences **18**, 434–447.

Ylianttila L, Visuri R, Huurto L, Jokela K. 2005. Evaluation of a single-monochromator diode array spectroradiometer for sunbed UV-radiation measurements. Photochemistry and Photobiology **81**, 333–41.

Zeiger E. 1984. Blue light and stomatal function. In: Senger H. (eds) blue light effects in biological systems. Proceedings in Life Sciences. Springer, Berlin, Heidelberg, .

Zeiger E, Iino M, Shimazaki KI, Ogawa T. 1987. The blue-light response of stomata: mechanism and function. Stomatal Function. Stanford University Press, 209–227.

Table 1. Light conditions for parent plants under solar radiation in the field and their offspring in growth chambers. A. Photosynthetically active radiation (PAR, 400-700 nm), blue (400 to 500 nm), UVA2 (340 to 400 nm), UVA1 (315 to 340 nm), UVB (280 to 315 nm). All values are shown as "min (mean) max". B. The light condition at peak PAR for 6 h and the UV-B lamps were turned on. The daily total PAR was 23.688 mol m^{-2} for all treatments. Values are mean ± standard error. The average estimated biologically effective UV doses for both experiments are shown in Supplemental table S4.

A. Light treatments for parental plants in the field (experimental period: early May to early June of 2016).

Light treatment	PAR (mol m^{-2} day^{-1})	Blue (mol m^{-2} day^{-1})	UVA (mol m^{-2} day^{-1})	UVB (mmol m^{-2} day^{-1})
$+UV_{parental}$	13.7 (41.88) 52.8	2.85 (8.41) 10.56	1.25 (3.32) 4.11	16.6 (45.9) 59.2
$–UV_{parental}$	14.4 (42.70) 53.8	2.91 (8.57) 10.76	0.74 (2.01) 2.50	0.003 (0.008) 0.01

B. Light treatments for the offspring in growth chambers.

Light treatment	PAR (µmol m^{-2} s^{-1})	Blue (µmol m^{-2} s^{-1})	UVA (µmol m^{-2} s^{-1})	UVB (µmol m^{-2} s^{-1})
1) UVB+Blue+	631 ± 6.4	95.5 ± 1.0	5.89 ± 0.17	3.19 ± 0.05
2) UVB+Blue−	634 ± 6.6	2.81 ± 0.03	5.85 ± 0.17	3.18 ± 0.06
3) UVB−Blue+	639 ± 8.6	96.7 ± 1.3	3.10 ± 0.08	0.007 ± 0.0032
4) UVB−Blue−	637 ± 9.0	2.82 ± 0.04	3.21 ± 0.15	0.004 ± 0.0014

Table 2. *P* values from ANOVA for morphological and physiological traits separately in Aurora and in ILB938. T is abbreviation for transgenerational effect of parental UV treatment. When the three-way interaction was significant, data was further analyzed separately by UVB's presence which is indicated inside the parenthesis. Specific stem length was not included, as all interactions including accession were not significant (see Supplementary Data Table S3). ANOVA for $M_{leaf/shoot}$ is the same as $M_{stem/shoot}$. Bold indicates $p \leq 0.05$. The row labelled 'Model' indicates the ANOVA weighting used, 1 = unweighted, 2 = weighted for unequal variance due to plant size, 3 = weighted for unequal variance due to plant size and light treatments.

In Aurora	Stem length	Leaf area	Shoot dry mass	$M_{stem/shoot}$	Specific leaf area	Stomatal conductance
Model	2)	1)	1)	1)	1)	2)
Blue	**<0.0001**	**<0.0001**	0.0007	**<0.0001**	**0.024**	**<0.0001**
UVB	**<0.0001**	**0.0001**	0.0007	**0.028**	**0.0011**	**0.0017**
T	0.17	0.18	0.30	0.18	0.62	0.79
Blue × UVB	0.60	0.20	0.46	0.69	0.69	0.17
Blue × T	0.18	0.088	0.057	**0.041**	0.68	0.92
UVB × T	0.78	0.39	0.32	0.57	0.97	0.46
Blue × UVB × T	0.073	0.060	**0.027**	0.31	0.66	0.73
Blue × T (UVB–)	–	–	**0.0054**	–	–	–
Blue × T (UVB+)	–	–	0.82	–	–	–

In ILB938	Stem length	Leaf area	Shoot dry mass	$M_{stem/shoot}$	Specific leaf area	Stomatal conductance
Model	3)	2)	2)	3)	1)	2)
Blue	**0.0002**	**0.0001**	**0.0006**	**<0.0001**	**0.0017**	**<0.0001**
UVB	**<0.0001**	**0.021**	**0.0042**	0.11	0.42	**<0.0001**
T	0.71	0.76	0.99	0.055	0.99	**0.0002**
Blue × UVB	0.86	**0.0004**	**0.011**	**0.038**	0.86	**0.020**
Blue × T	**0.016**	**0.0015**	**0.017**	0.14	0.87	0.41
UVB × T	0.89	0.44	0.72	0.74	0.86	0.67

Blue × UVB × T	0.58	0.25	0.69	0.34	0.35	0.62

1

Table 3. Flavonoid and phenolic acid compounds measured with HPLC-MS^n in the leaves of accessions Aurora and ILB938 of *Vicia faba*, their abbreviations, retention time (RT), molecular mass (M+1), and weightings in principal component analysis (PC1, PC2 and PC3, with explained percentage of variance between parenthesis) for kaempferols and quercetins separately; bold indicates absolute value ≧0.5. Flavonoid compounds are listed sequentially by molecular mass.

Kaempferol glycosides	Abbreviation	RT (min)	M+1 (g mol^{-1})	PC1 (86.5)	PC2 (6.2)	PC3 (3.5)
Kaempferol-3-*O*-arabinoside-7-*O*-rhamnoside	K2-1	21.17	564.62	0.305	-0.100	0.067
Kaempferol-3-*O*-rhamnoside-7-*O*-rhamnoside	K2-2	17.07	578.54	0.251	-0.288	**0.541**
Kaempferol-3-*O*-rhamnoglucoside	K2-3	16.03	594.54	0.196	**-0.803**	0.035
Kaempferol-3-*O*-rhamnogalactoside	K2-4	15.29	594.54	0.306	-0.110	**-0.528**
Kaempferol-3-*O*-acetyl-galactoside-7-*O*-rhamnoside	K2-5(acetyl)	18.52	636.59	-0.308	-0.074	-0.072
Kaempferol-3-*O*-acetyl-rhamnogalactoside	K2-6(acetyl)	19.30	636.59	-0.308	-0.074	-0.068
Kaempferol-3-*O*-rhamnoarabinoside-7-*O*-rhamnoside	K3-1	11.87	710.77	-0.293	0.006	-0.251
Kaempferol-3-*O*-rhamnogalactoside-7-*O*-rhamnoside	K3-2	8.02	740.70	-0.249	-0.416	**0.559**
Kaempferol-3-*O*-rhamnoglucoside-7-*O*-rhamnoside	K3-3	8.43/8.65	740.70	-0.303	-0.160	0.102
kaempferol-3-*O*-rhamnoglucoside-7-*O*-glucoside	K3-4	7.18	756.70	-0.308	-0.074	-0.065
Kaempferol-3-*O*-acetyl-rhamnogalactoside-7-*O*-rhamnoside	K3-5(acetyl)	13.81	782.76	-0.304	-0.175	0.145
Kaempferol-3-*O*-rhamnoglucoside-7-*O*-rhamnoside-4'-rhamnoside	K4-1	7.90	886.85	-0.308	-0.072	-0.046

Quercetin glycosides	Abbreviation	RT (min)	M+1 (g mol^{-1})	PC1 (75.0)	PC2 (16.9)	PC3 (4.5)	1
Quercetin-3-*O*-rhamnoside-7-*O*-arabinoside	Q2-1	11.57	580.62	0.230	**-0.644**	0.128	
Quercetin-3-*O*-rhamnoglucoside	Q2-2	10.56	610.55	0.224	**-0.655**	0.097	
Quercetin-3-*O*-rhamnoarabinoside-7-*O*-rhamnoside	Q3-1	10.07	726.78	-0.360	-0.148	0.123	
Quercetin-3-*O*-rhamnogalactoside-7-*O*-rhamnoside	Q3-2	7.25	756.70	-0.376	-0.079	0.135	
Quercetin-3-*O*-rhamnoglucoside-7-*O*-rhamnoside	Q3-3	7.45/7.61	756.70	-0.379	-0.100	0.087	
Quercetin-3-*O*-rhamnorhamnoglucoside	Q3-4	11.03	756.70	-0.286	-0.262	**-0.912**	
Quercetin-3-*O*-rhamnoglucoside-7-*O*-glucoside	Q3-5	5.66	772.70	-0.369	0.036	0.119	
Quercetin-3-*O*-acetyl-rhamnogalactoside-7-*O*-rhamnoside	Q3-6(acetyl)	10.86	798.75	-0.370	-0.153	0.120	
Quercetin-3-*O*-acetyl-rhamnoglucoside-7-*O*-rhamnoside	Q3-7(acetyl)	12.17	798.75	-0.356	-0.157	0.270	

Phenolic acid compounds	RT (min)	M+1 (g mol^{-1})
Caffeoylmalic-acid	9.44	296.23
Coumaroylglucoside	5.90	326.30
Feruloylglucoside	**6.58**	356.33

Table 4. *P* values from the ANOVA analysis for the effects of transgenerational effect (T), offspring blue, and UVB treatments and their interactions on total kaempferol, K[di], K[ace.tri.tetra], total quercetin, Q[di] and Q[ace.tri]. Bold indicates $p \leq 0.05$.

Compound group	Accession	T	Blue	UVB	T × Blue	T × UVB	Blue × UVB	T × Blue × UVB
Total Kaempferol	Aurora	0.81	**<0.0001**	0.017	0.11	0.32	0.16	0.64
	ILB938	0.64	**<0.0001**	**0.0005**	0.66	0.70	0.43	0.52
K[di]	Aurora	0.34	**0.0017**	0.77	0.71	0.19	0.32	0.59
	ILB938	0.71	**<0.0001**	**0.0006**	0.60	0.65	0.40	0.52
K[ace.tri.tetra]	Aurora	0.088	**<0.0001**	**0.0008**	0.14	0.33	0.094	0.97
	ILB938	0.45	**0.0001**	**0.0007**	0.20	0.55	**0.021**	0.56
Total Quercetin	Aurora	0.38	**<0.0001**	**<0.0001**	0.41	**0.0005**	**0.0003**	0.31
	ILB938	0.69	**<0.0001**	**<0.0001**	0.57	0.89	**<0.0001**	0.26
Q[di]	Aurora	0.20	0.12	**0.0001**	0.13	0.087	**0.044**	0.068
	ILB938	0.42	**<0.0001**	**<0.0001**	0.68	0.83	**<0.0001**	0.29
Q[ace.tri]	Aurora	0.21	**<0.0001**	**<0.0001**	0.19	**0.0034**	**0.0009**	0.67
	ILB938	0.55	0.38	**0.04**	0.10	0.47	**<0.0001**	0.72

Kaempferols were grouped into K[di] and K[ace.tri.tetra] according to PCA analysis. K[di] is K2-1, K2-2, K2-3 and K2-4. K[ace.tri.tetra] is K2-5(acetyl), K2-6(acetyl), K3-1, K3-2, K3-3, K3-4, K3-5(acetyl) and K4-1. Quercetins were grouped into Q[di] and Q[ace.tri] according to PCA analysis. Q[di] is Q2-1 and Q2-2. Q[ace.tri] is Q3-1, Q3-2, Q3-3, Q3-4, Q3-5, Q3-6(acetyl) and Q3-7(acetyl). The full names of all compounds are in Table 4.

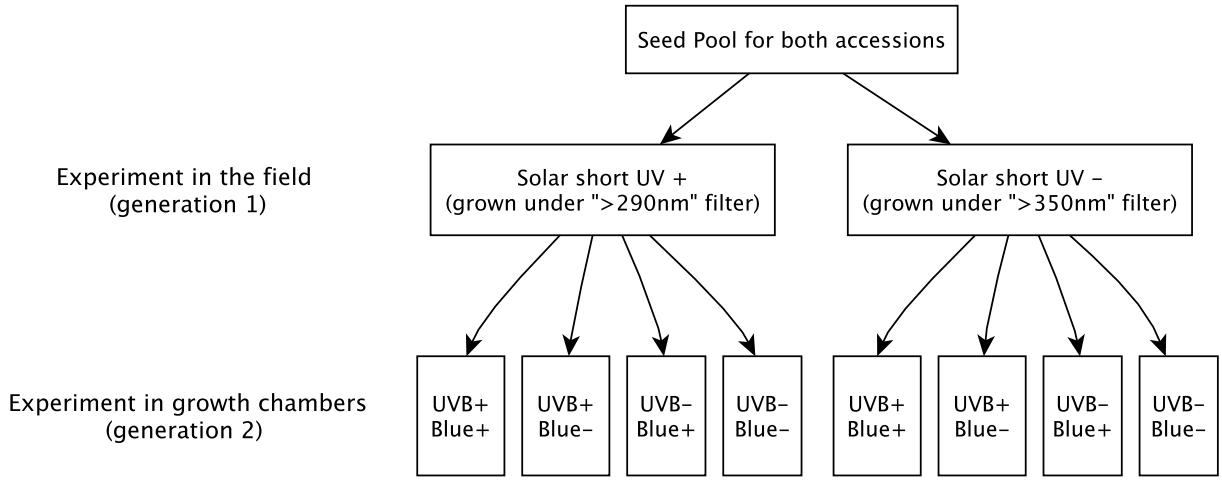

1

2 **Fig. 1.** Scheme of experimental design for the present experiment (experiment in growth
3 chambers). The two parental treatments derived from generation 1: they were grown under two
4 filter treatments in the field. The current generation (generation 2) were exposed to four light
5 treatments in growth chambers.

6

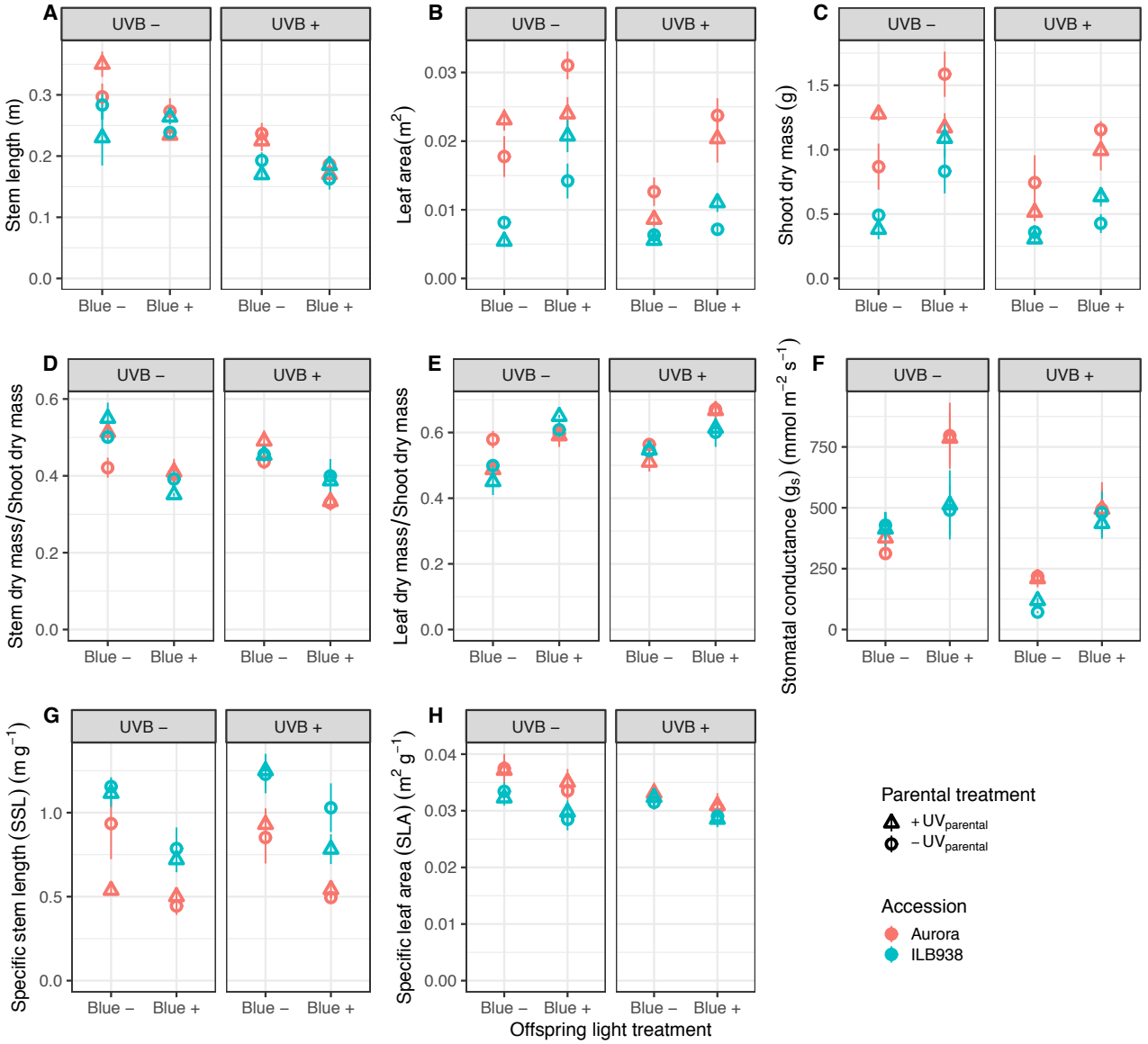

Fig. 2. Morphological traits and stomatal conductance of plants in a factorial experiment with two parental treatments (+$UV_{parental}$, –$UV_{parental}$), two *Vicia faba* accessions (Aurora and ILB938) and four offspring light treatments (UVB–Blue–, UVB–Blue+, UVB+Blue–, UVB+Blue+). (A) Stem length; (B) leaf area per plant; (C) shoot dry mass per plant; (D) stem dry mass/shoot dry mass; (E) leaf dry mass/shoot dry; (F) abaxial leaf stomatal conductance; (G) specific stem length (SSL); (H) specific leaf area (SLA). All traits were measured at 28 days after sowing, except stomatal conductance that was measured at 27 d. Values are means ± SE of four replicates. ANOVA results are shown in Supplementary Data Table S3 and Table 2.

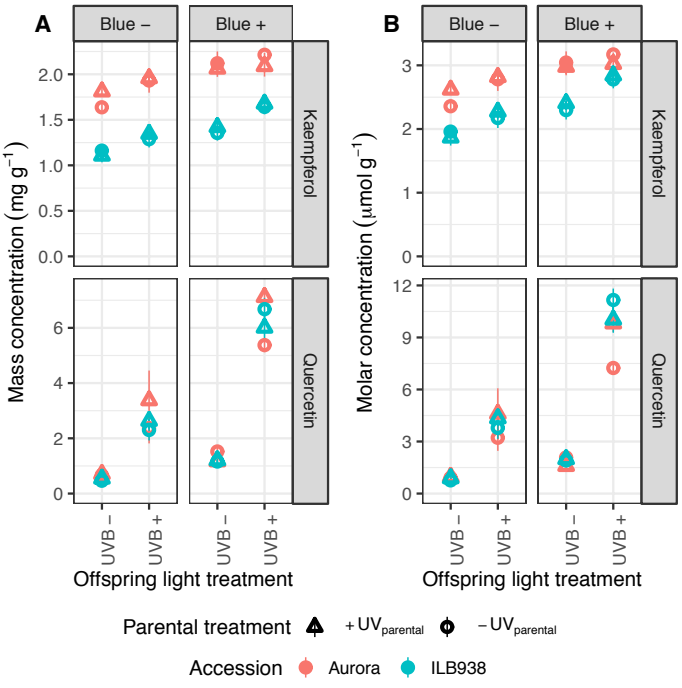

Fig. 3. Whole-leaf concentration of total kaempferols and quercetins per unit leaf dry mass of the youngest fully expanded leaves of plants in a factorial experiment with two parental treatments (+UV$_{parental}$, –UV$_{parental}$), two *Vicia faba* accessions (Aurora and ILB938) and four offspring light treatments (UVB–Blue–, UVB+Blue–, UVB–Blue+, UVB+Blue+). (A) mass (mg g^{-1}) concentration of total kaempferols and quercetins; (B) molar (µmol g^{-1}) concentration of total kaempferols and quercetins. Values are means ± SE of four replicates.

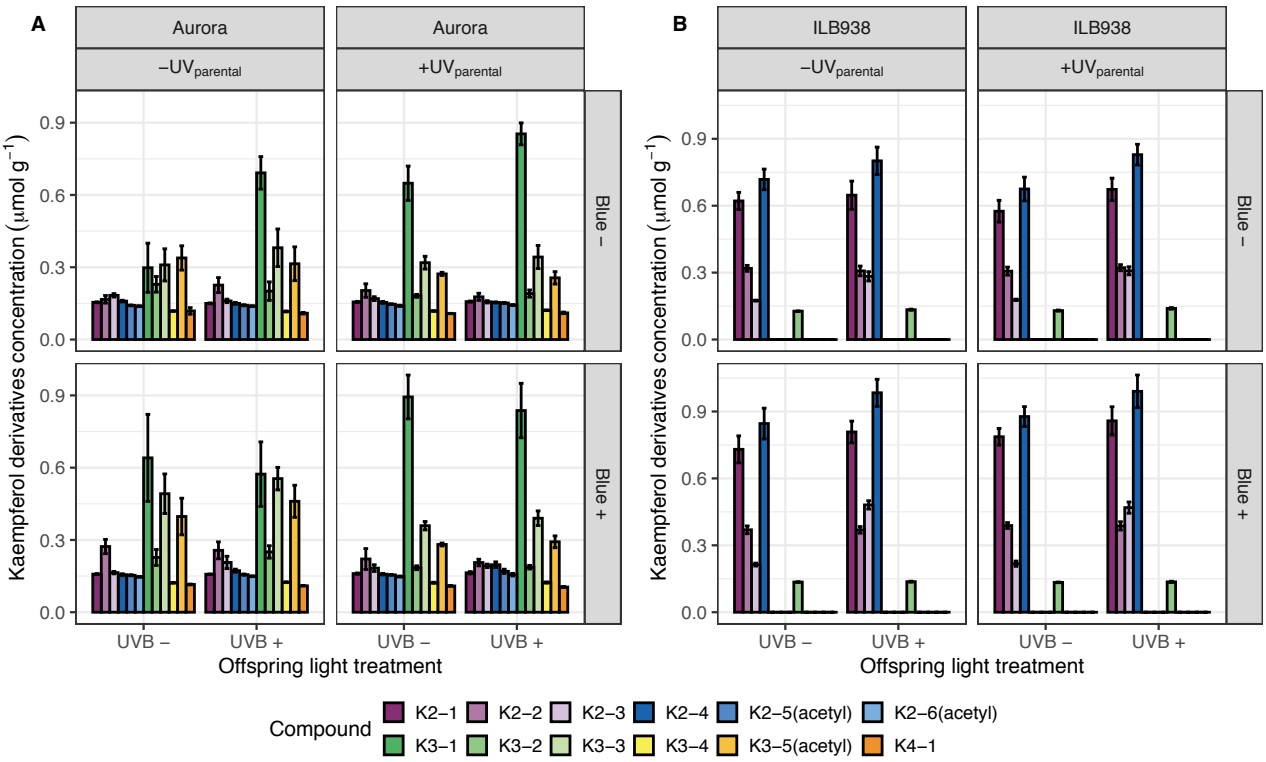

Fig. 4. Kaempferol profiles of plants in a factorial experiment with two parental treatments ((+$UV_{parental}$, –$UV_{parental}$), two *Vicia faba* accessions (Aurora and ILB938) and four offspring light treatments (UVB–Blue–, UVB+Blue–, UVB–Blue+, UVB+Blue+). (A) molar concentration (µmol g^{-1}) of individual kaempferol glycosides per unit leaf dry mass in Aurora; (B) molar concentration (µmol g^{-1}) of individual kaempferol glycosides per unit leaf dry mass in ILB938. Values are means ± SE of four replicates.

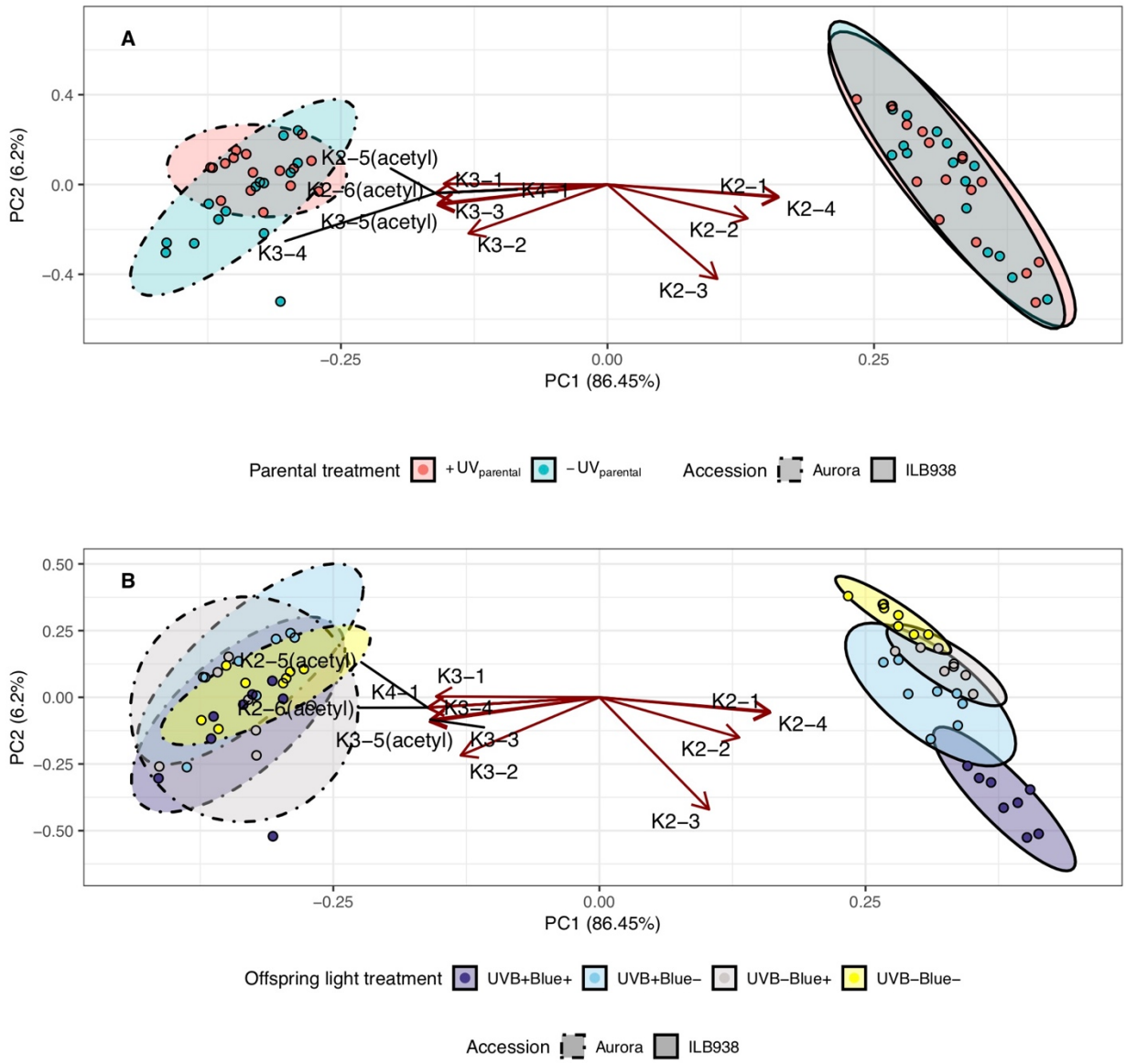

Fig. 5. Principal component analysis (PCA) of the kaempferol glycosides profile of plants in a factorial experiment with two parental treatments (+$UV_{parental}$, –$UV_{parental}$), two *Vicia faba* accessions (Aurora and ILB938) and four offspring light treatments (UVB–Blue–, UVB+Blue–, UVB–Blue+, UVB+Blue+). The ellipses show 0.95 confidence regions assuming bivariate t distribution. The first two principal components (PC1 and PC2) explain together 92.7% of the total variation. (A) PCA (PC1 vs. PC2) of the kaempferol glycosides profile plotted with accession × parental UV treatment; (B) PCA (PC1 vs. PC2) of the kaempferol glycosides profile plotted with accession × offspring light treatment. All kaempferol compounds are shown with labels, their full names and rotation values for PC1 and PC2 are in Table 4.

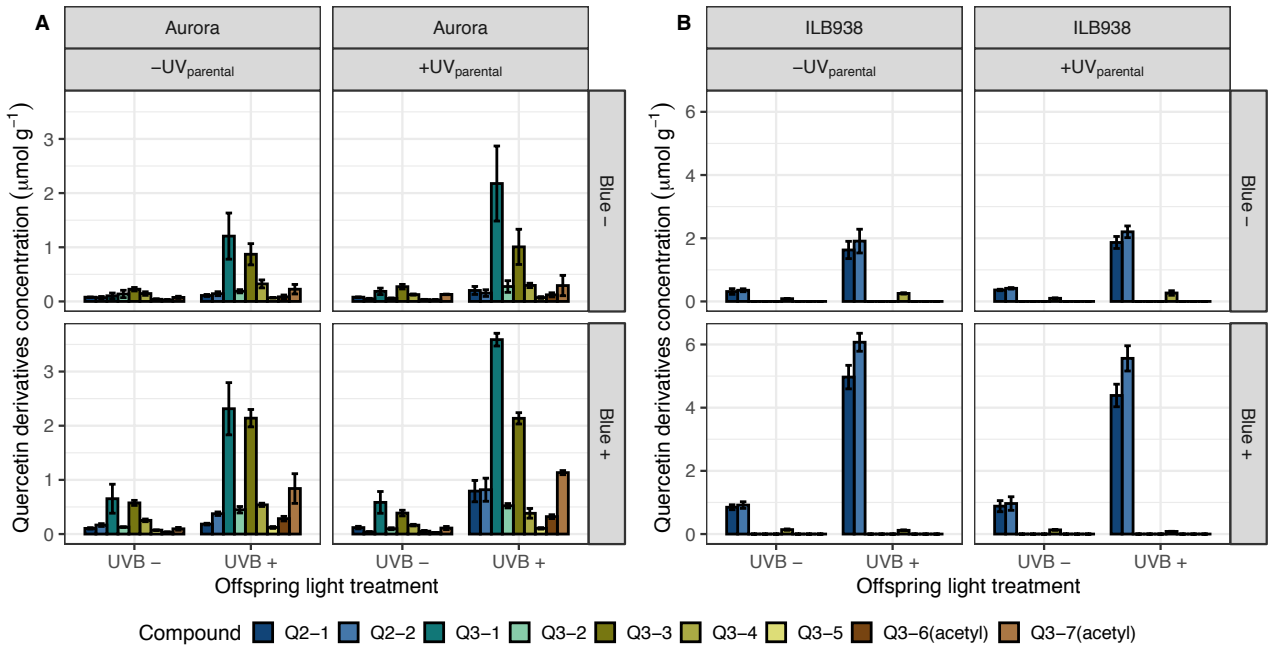

Fig. 6. Quercetin profiles of plants in a factorial experiment with two parental treatments ($+UV_{parental}$, $-UV_{parental}$), two *Vicia faba* accessions (Aurora and ILB938) and four offspring light treatments (UVB–Blue–, UVB+Blue–, UVB–Blue+, UVB+Blue+). (A) molar concentration (µmol g^{-1}) of individual quercetin glycosides per unit leaf dry mass in Aurora; (B) molar concentration (µmol g^{-1}) of individual quercetin glycosides per unit leaf dry mass in ILB938. All values are means ± SE of four replicates.

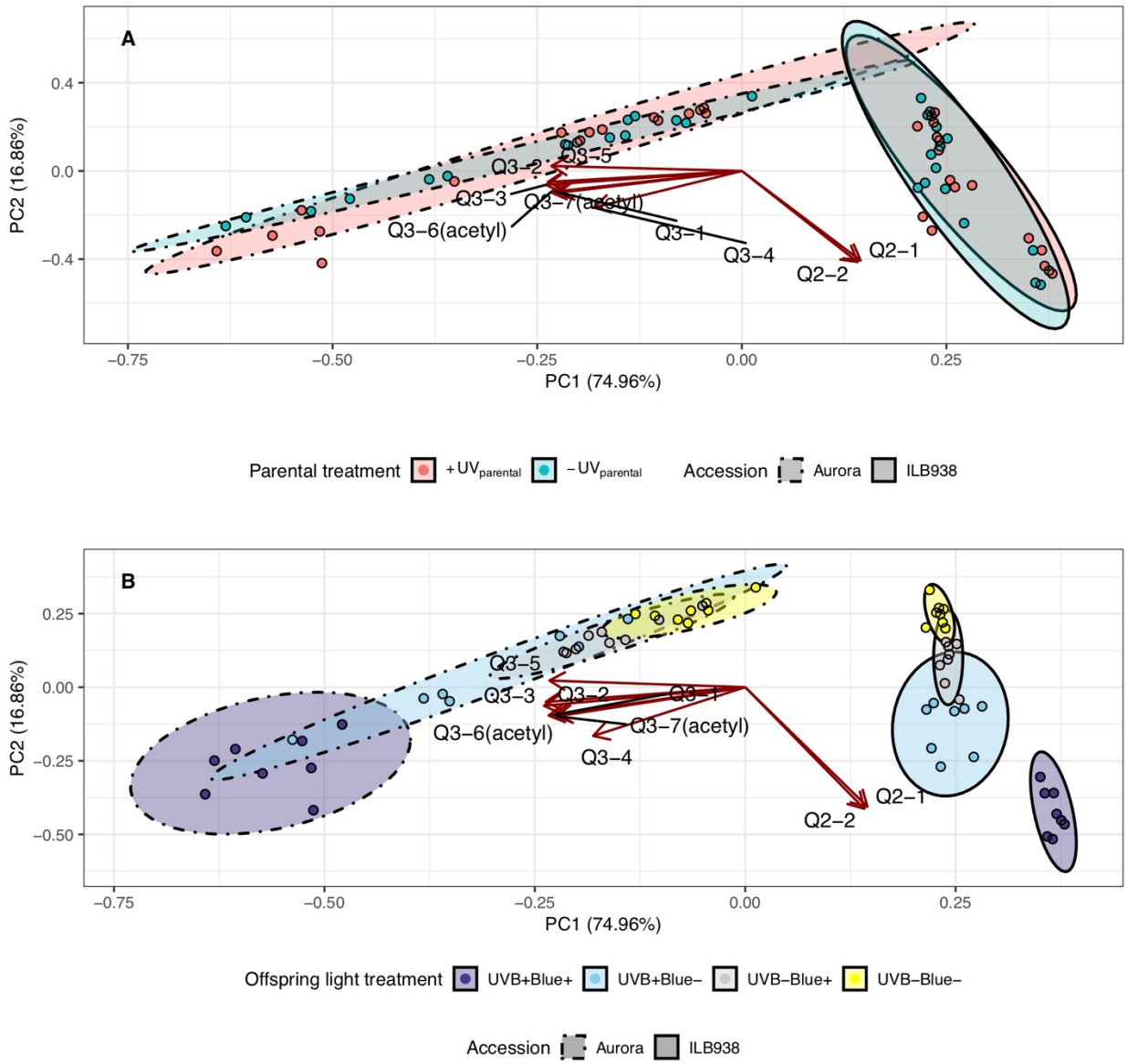

Fig. 7. Principal component analysis (PCA) of the quercetin glycosides profile of plants in a factorial experiment with two parental treatments (+$UV_{parental}$, –$UV_{parental}$), two *Vicia faba* accessions (Aurora and ILB938) and four offspring light treatments (UVB–Blue–, UVB+Blue–, UVB–Blue+, UVB+Blue+). The ellipses show 0.95 confidence regions assuming bivariate t distribution. The first two principal components (PC1 and PC2) explain together 91.8 % of the total variation. (A) PCA (PC1 vs. PC2) of the quercetin glycosides profile plotted with accession × parental UV treatment; (B) PCA (PC1 vs. PC2) of the quercetin glycosides profile plotted with accession × offspring light treatment. Quercetin compounds are shown with labels, their full names and rotation values for PC1 and PC2 are in Table 4.

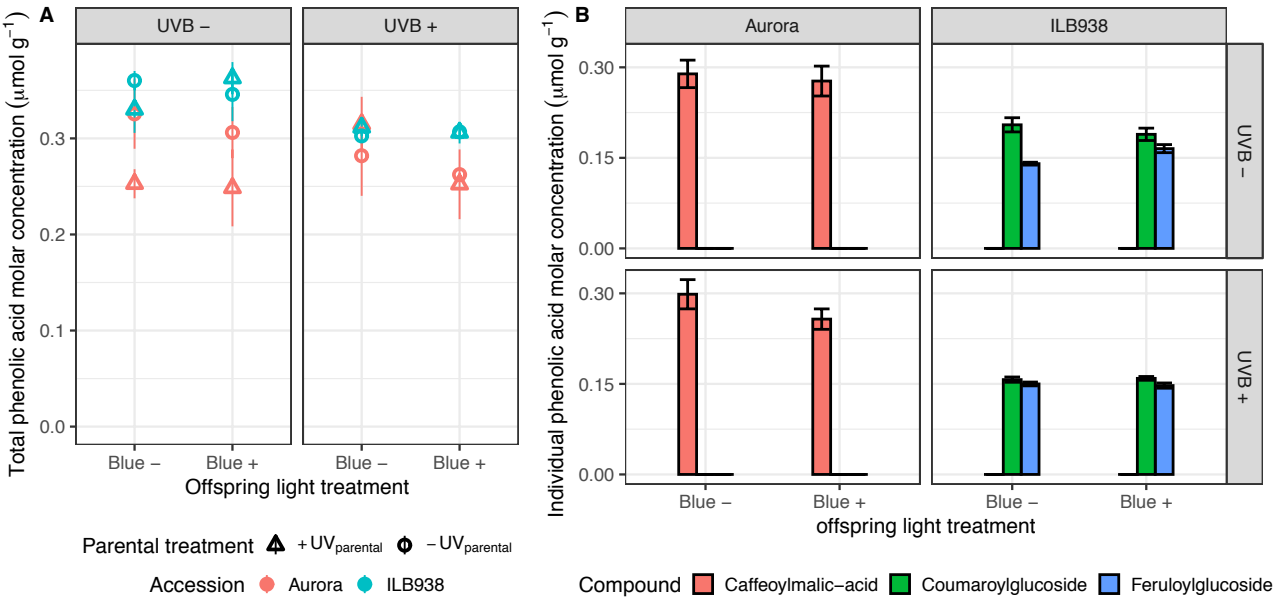

Fig. 8. Phenolic acids of the youngest fully expanded leaves of plants in a factorial experiment with two parental treatments (+$UV_{parental}$, –$UV_{parental}$), two *Vicia faba* accessions (Aurora and ILB938) and four offspring light treatments (UVB–Blue–, UVB+Blue–, UVB–Blue+, UVB+Blue+). (A) Whole-leaf molar concentration (µmol g^{-1}) of total phenolic acids per unit leaf dry mass; (B) Whole-leaf molar concentration (µmol g^{-1}) of individual phenolic acid compounds per unit leaf dry mass. Values are means ± SE of four replicates.

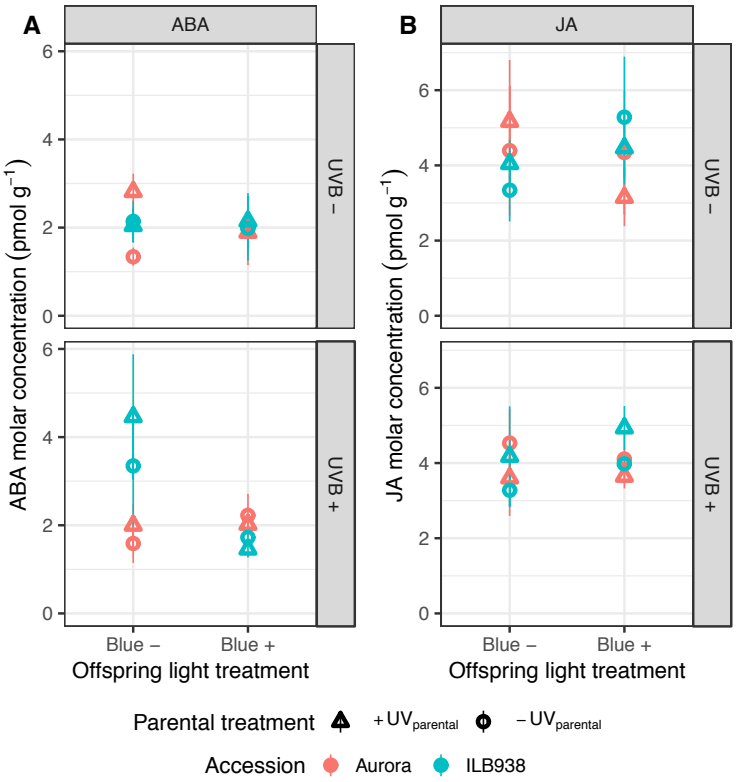

Fig. 9. Whole-leaf molar concentration (µmol g^{-1}) of phytohormone of plants in a factorial experiment with two parental treatments (+UV$_{parental}$, –UV$_{parental}$), two *Vicia faba* accessions (Aurora and ILB938) and four offspring light treatments (UVB–Blue–, UVB+Blue–, UVB–Blue+, UVB+Blue+). (A) molar concentration of abscisic acid (ABA) per unit leaf dry mass; (B) molar concentration of jasmonic acid (JA) per unit leaf dry mass. Values are means ± SE of four replicates.

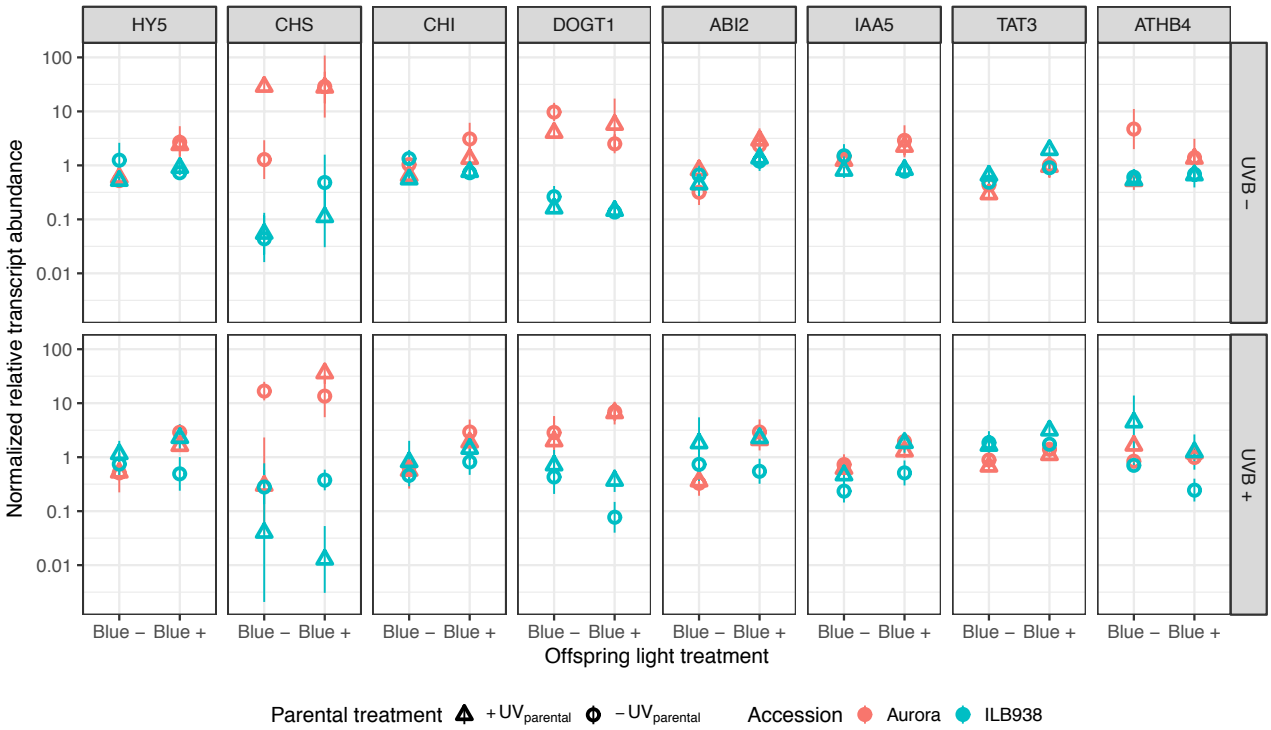

Fig. 10. Normalized relative transcript abundance scaled to average expression of all genes in each run: HY5, CHS, CHI, DOGT1, ABI2, IAA5, TAT3 and ATHB4 of plants in a factorial experiment with two parental treatments (+$UV_{parental}$, –$UV_{parental}$), two *Vicia faba* accessions (Aurora and ILB938) and four offspring light treatments (UVB–Blue–, UVB+Blue–, UVB–Blue+, UVB+Blue+). Values are plotted on a logarithmic scale with means ± SE of four replicates computed using log_{10} transformed data.

1

1

SUPPLEMENTARY DATA

Supplementary data are available online and consist of the following. Figure S1: The figure shows stem-to-shoot dry mass ratio was unrelated to shoot dry mass. Figure S2: Absorbance of epidermal flavonoids per unit area on 27 d after sowing. Figure S3: Epidermal chlorophyll content per unit area on 27 d after sowing. Figure S4: Principal component analysis (PCA) of the kaempferol glycosides profile (PC1 v.s. PC3). Figure S5: Principal component analysis (PCA) of the quercetin glycosides profile (PC1 v.s. PC3). Table S1: Number of plants for four replicates per treatment per accession. Table S2: Genes chosen for q-PCR analysis and the corresponding primers. Table S3: *P* values from ANOVA for morphological and physiological traits.

Supplementary Data

- **Supplemental figures**

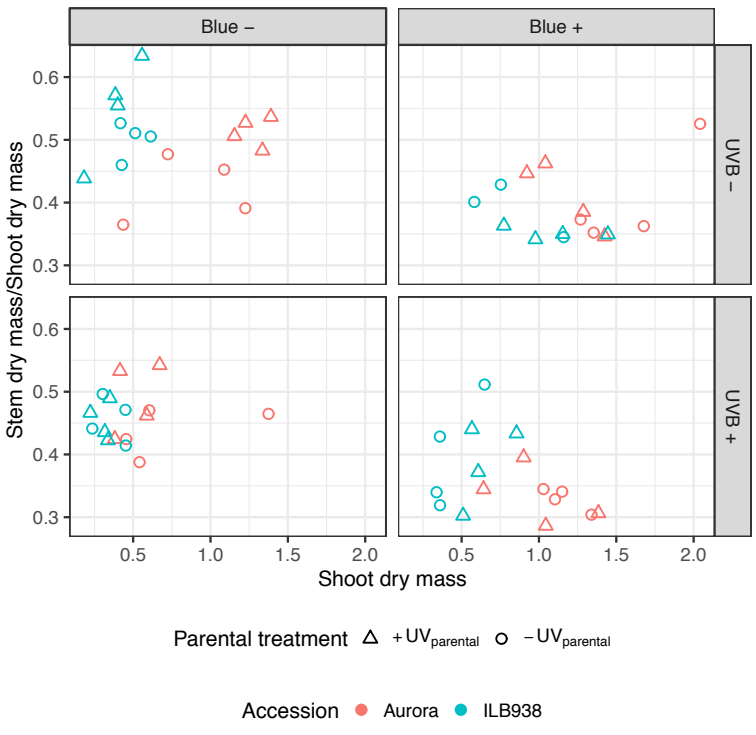

Figure S1. Stem-to-shoot dry mass ratio was unrelated ($p > 0.09$) to shoot dry mass in a factorial experiment with two parental treatments (+$UV_{parental}$, –$UV_{parental}$), two *Vicia faba* accessions (Aurora and ILB938), and four offspring light treatments (UVB–Blue–, UVB+Blue–, UVB–Blue+, UVB+Blue+).

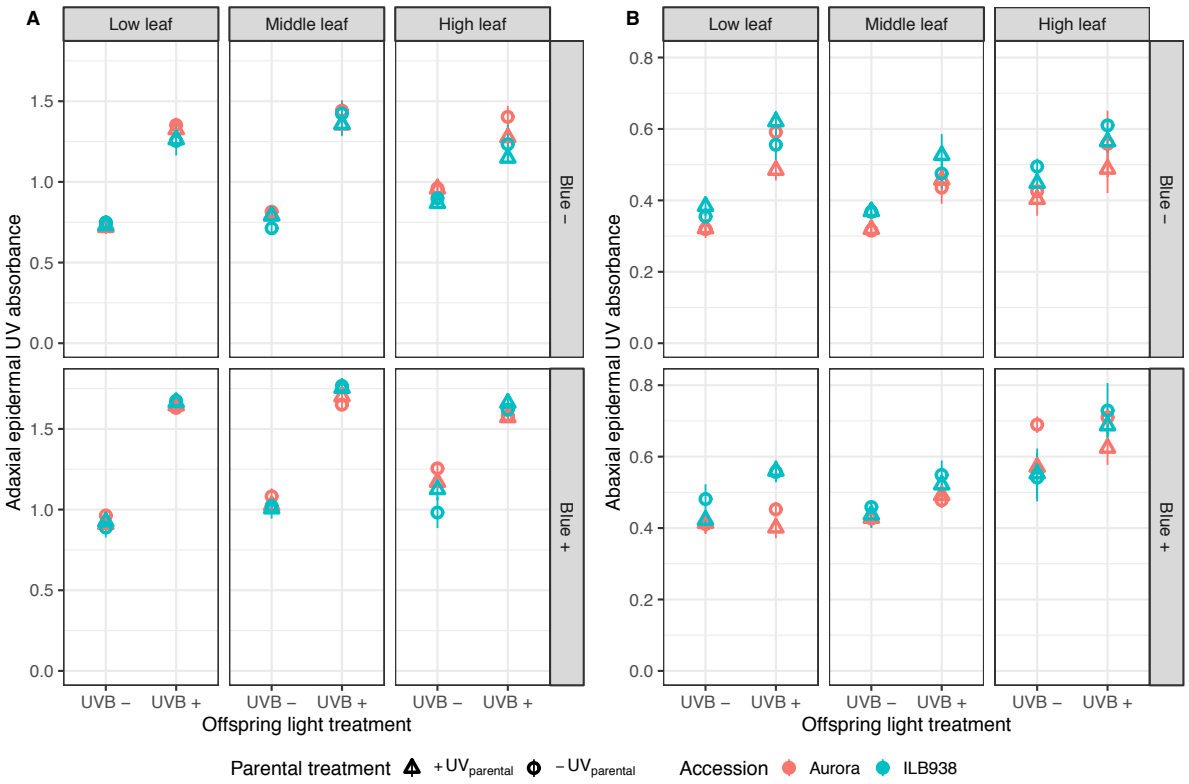

Figure S2. Absorbance of epidermal flavonoids per unit area of plants assessed using Dualex on 27 d after sowing in a factorial experiment with two parental treatments (+$UV_{parental}$, –$UV_{parental}$), two *Vicia faba* accessions (Aurora and ILB938), and four offspring light treatments (UVB–Blue–, UVB+Blue–, UVB–Blue+, UVB+Blue+). (A) Adaxial epidermis absorbance of epidermal flavonoids; (B) Abaxial epidermis absorbance of epidermal flavonoids. Leaves at three positions were measured: "Low leaf" is leaf at the bottom of the plant; "Middle leaf" is leaf located at 50% height of the plant; "High leaf" is the youngest fully expanded leaf. Values are means ±SE of four replicates. The youngest expanded leaves measured for the first time on the last date were harvested on the next day for phenolic analysis by HPLC.

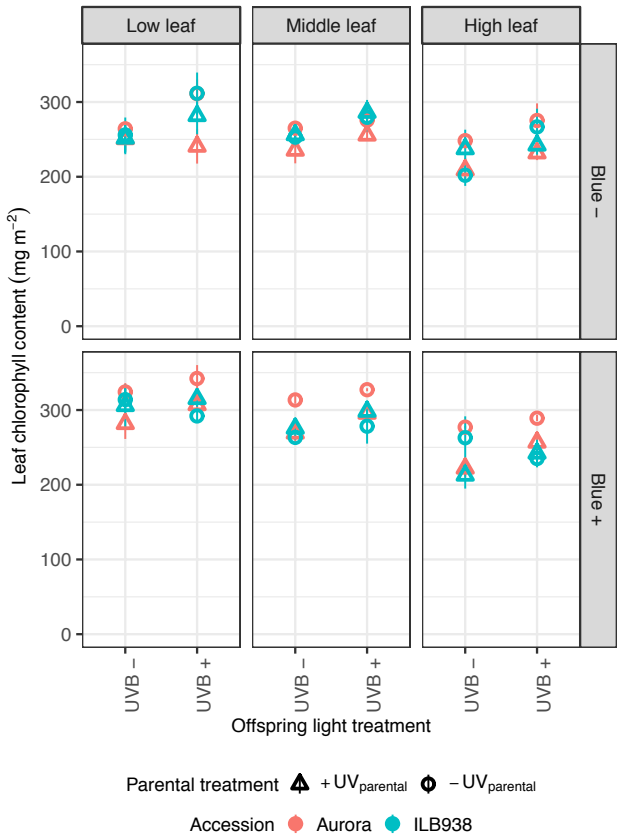

Figure S3. Epidermal chlorophyll content per unit area of plants assessed using Dualex on 27 d after sowing in a factorial experiment with two parental treatments (+UV$_{parental}$, –UV$_{parental}$), two *Vicia faba* accessions (Aurora and ILB938), and four offspring light treatments (UVB–Blue–, UVB+Blue–, UVB–Blue+, UVB+Blue+). Leaves at three positions were measured: "Low leaf" is leaf at the bottom of the plant; "Middle leaf" is leaf located at 50% height of the plant; "High leaf" is the youngest fully expanded leaf. Values are means ±SE of four replicates.

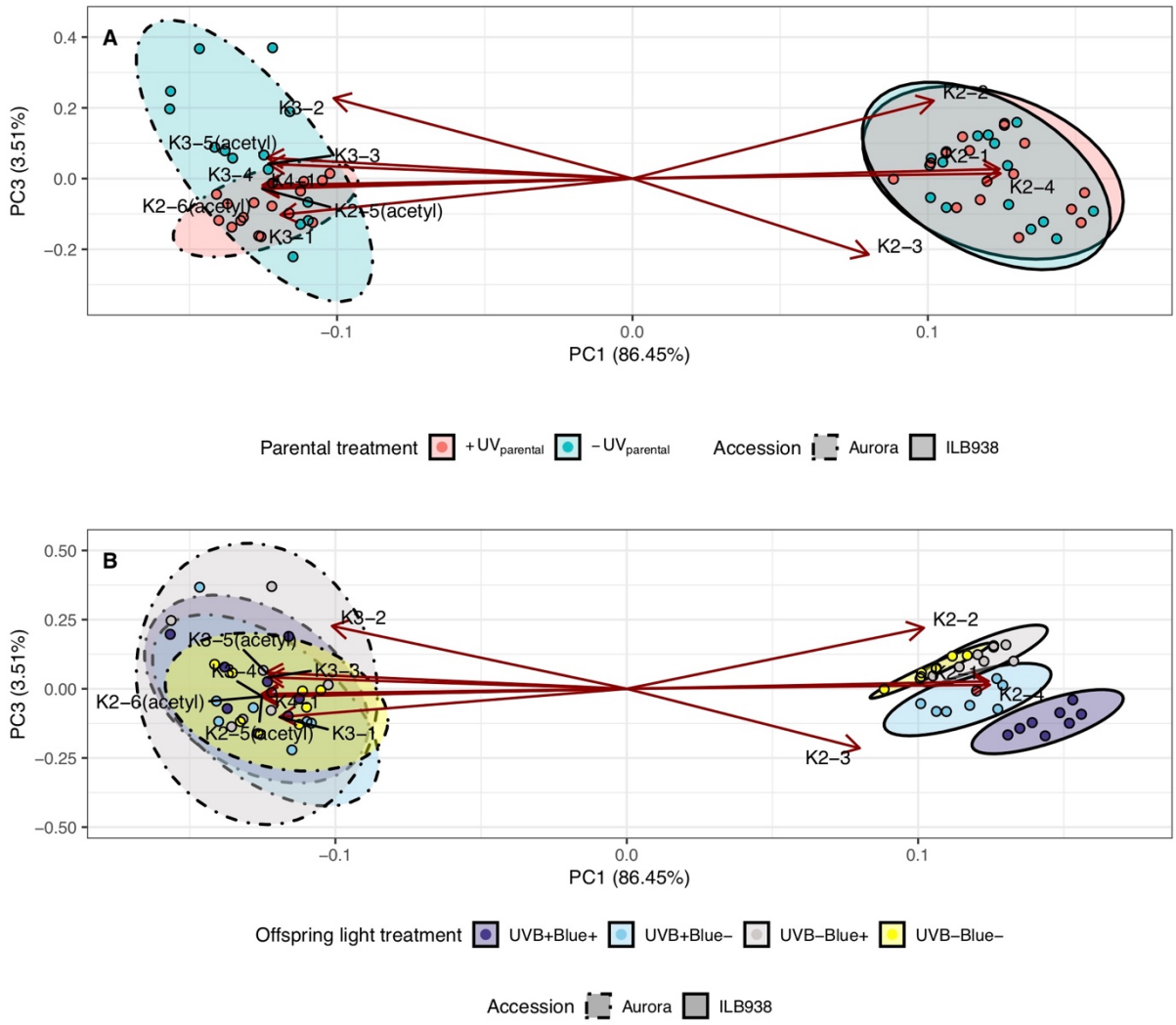

Figure S4. Principal component analysis (PCA) of the kaempferol glycosides profile of plants in a factorial experiment with two parental treatments (+$UV_{parental}$, –$UV_{parental}$), two *Vicia faba* accessions (Aurora and ILB938), and four offspring light treatments (UVB–Blue–, UVB+Blue–, UVB–Blue+, UVB+Blue+). The ellipses show 0.95 confidence regions assuming bivariate t distribution. The first and third principal components (PC1 and PC3) explain together *90.0*% of the total variation. (A) PCA (PC1 vs. PC3) of the kaempferol glycosides profile plotted with accession × parental UV treatment; (B) PCA (PC1 vs. PC3) of the kaempferol glycosides profile plotted with accession × offspring light treatment. All kaempferol compounds are shown with labels, their full names and rotation values for PC1 and PC3 are shown in Table 4.

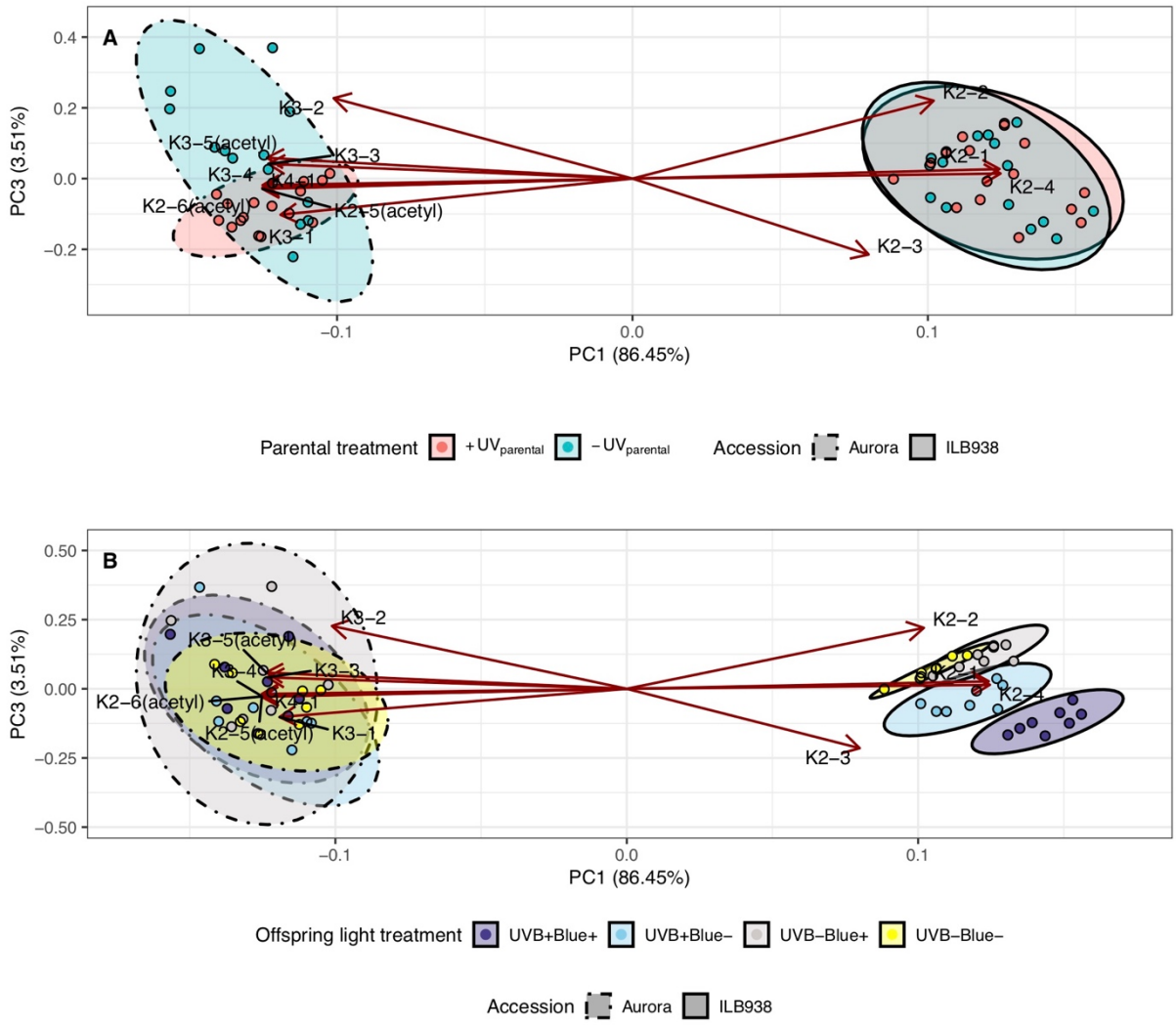

Figure S5. Principal component analysis (PCA) of the quercetin glycosides profile of plants in a factorial experiment with two parental treatments (+$UV_{parental}$, –$UV_{parental}$), two *Vicia faba* accessions (Aurora and ILB938), and four offspring light treatments (UVB–Blue–, UVB+Blue–, UVB–Blue+, UVB+Blue+). The ellipses show 0.95 confidence regions assuming bivariate t distribution. The first and third principal components (PC1 and PC3) explain together 79.5% of the total variation. A. PCA (PC1 vs. PC3) of the quercetin glycosides profile plotted with accessions × parental UV treatments; B. PCA (PC1 vs. PC3) of the quercetin glycosides profile plotted with accessions × offspring light treatments. All quercetin compounds are shown with labels, their full names and rotation values for PC1 and PC3 are shown in Table 4.

- **Supplementary Tables**

Supplementary Table S1. Number of plants for four replicates per treatment per accession.

Replicate	Accession	UVB+Blue+	UVB+Blue−	UVB−Blue+	UVB−Blue−
Replicate 1	Aurora (+$UV_{parental}$)	3	2	3	3
	Aurora (–$UV_{parental}$)	2	2	1	2
	ILB938 (+$UV_{parental}$)	3	3	3	3
	ILB938 (–$UV_{parental}$)	2	2	2	2
Replicate 2	Aurora (+$UV_{parental}$)	3	4	3	2
	Aurora (–$UV_{parental}$)	3	2	3	1
	ILB938 (+$UV_{parental}$)	3	3	3	3
	ILB938 (–$UV_{parental}$)	2	1	2	3
Replicate 3	Aurora (+$UV_{parental}$)	4	3	3	2
	Aurora (–$UV_{parental}$)	2	3	3	3
	ILB938 (+$UV_{parental}$)	3	2	2	3
	ILB938 (–$UV_{parental}$)	2	2	1	3
Replicate 4	Aurora (+$UV_{parental}$)	5	4	3	3
	Aurora (–$UV_{parental}$)	3	3	3	3
	ILB938 (+$UV_{parental}$)	2	3	3	3
	ILB938 (–$UV_{parental}$)	1	1	3	3

Supplementary Table S2. Genes chosen for q-PCR analysis, primers designed to quantify these genes, and the function of the gene products.

Primers	Sequence (5′ → 3′)	Gene name	Gene product function
HY5 for	GAGGGAGAGGAAAAAG	ELONGATED	basic leucine zipper (bZIP)
HY5 rev	GCATA	HYPOCOTYL5	transcription factor, involved
	GCTCGCAGTTGTGTTCT		in light-regulated
	TCA		transcriptional activation.
CHS for	CAGAGGCTGAGTCTGCA	CHALCONE SYNTHASE	chalcone synthase, a key
CHS rev	GTT		enzyme in biosynthesis
	GCCAGACTCTGTTTTGC		pathway of flavonoids
	TGC		
CHI for	CCGTTCCACCAGCAAAA	CHALCONE	chalcone isomerase, catalyzes
CHI rev	CAG	ISOMERASE	the conversion of chalcone to
	GCCAGACTCTGTTTTGC		flavanones
	TGC		

DOGT1 for DOGT1 rev	GGTTGGGCTCCTCAGTTGTT GGCCATGTAACCATTGGCAC	DON-GLUCOSYLTRANSFERASE 1	a DON-Glucosyltransferase, having quercetin glucosyltransferase activity
ABI2 for ABI2 rev	AGAGGACTGACAGTGAAATCGAA GTTTGAGTCCTGCGGCAAAG	ABA INSENSITIVE 2	protein phosphatase 2C, which negatively regulates abscisic acid-activated signaling pathway
IAA5 for IAA5 rev	AGGATGGTGATTGGATGCTC TTTCCATAGCTCGAGGTGCT	AUXIN-INDUCIBLE 2-27	transcription factor that is involved in auxin-activated signaling pathway
TAT3 for TAT3 rev	CAGCAAAAATGCTTGGAACA CTCCCATAGGCACAAAAGGA	TYROSINE AMINOTRANSFERASE 3	tyrosine aminotransferase that responds to jasmonic acid and wounding
ATHB4 for ATHB4 rev	TTGAGAGGGCTTCGTGTTCT TCTTCCAGCAACAACGACTG	HOMEOBOX-LEUCINE ZIPPER PROTEIN 4	homeodomain protein whose expression depends on phyB for red and far-red light response, which is involved in the shade avoidance syndrome.
Reference genes	Sequence (5′ → 3′)	Gene name	
ELF1A for ELF1A rev	GTGAAGCCCGGTATGCTTGT CTTGAGATCCTTGACTGCAACATT	eukaryotic elongation factor 1-alpha	

CYP2 for	TGCCGATGTCACTCCCA	cyclophilin 20-3
CYP2 rev	GAA	
	CAGCGAACTTGGAACCG	
	TAGA	

1
2

Supplementary Table S3. *P* values from ANOVA for morphological and physiological traits. T indicates for transgenerational effec of parental UV treatment; A indicates accession. ANOVA for $M_{leaf/shoot}$ is same as $M_{stem/shoot}$. Bold indicates $p \leq 0.05$. The row labelled 'Model' indicates the ANOVA weighting used, 1 = unweighted, 2 = weighted for unequal variance due to plant size, 3 = weighted for unequal variance due to plant size and light treatments.

	Stem length	Leaf area	Shoot dry mass	$M_{stem/shoot}$	Specific stem length	Specific leaf area	Stomatal conductance
Model	3)	2)	2)	1)	2)	1)	2)
Blue	0.078	**<0.0001**	**<0.0001**	**<0.0001**	**<0.0001**	**0.0002**	**<0.0001**
UVB	**<0.0001**	**0.0002**	**<0.0001**	**0.020**	**<0.0001**	**0.0008**	**<0.0001**
A	**0.012**	**<0.0001**	**<0.0001**	0.15	**<0.0001**	**0.0001**	**<0.0001**
T	0.48	0.25	0.61	0.17	0.96	0.77	**0.0002**
Blue × UVB	0.73	**0.0007**	**0.040**	0.69	**0.0034**	0.74	0.28
Blue × A	**0.0032**	**0.0031**	0.24	0.66	0.051	0.66	0.96
UVB × A	0.90	**0.0034**	0.19	0.55	0.92	**0.026**	**0.020**
Blue × T	0.51	**0.0068**	0.14	**0.031**	**0.0053**	0.69	0.43
UVB × T	0.80	0.59	0.93	0.55	0.85	0.90	0.98
A × T	0.15	0.066	0.16	0.12	0.12	0.67	0.25
Blue × UVB × A	0.59	**0.0069**	0.071	**0.0031**	0.27	0.82	**0.015**
Blue × UVB × T	0.45	0.94	0.41	0.29	**0.018**	0.37	0.96
Blue × A × T	**0.017**	**0.019**	**0.030**	0.73	0.064	0.81	0.58
UVB × A × T	0.88	0.095	0.12	0.87	0.29	0.85	0.36
Blue × UVB × A × T	0.11	**0.036**	**0.049**	0.68	0.56	0.82	0.59

3
4
5
6
7
8
9
10
11

Supplementary Table S4. Average estimated biologically effective UV doses calculated with five BSWFs (biological spectral weighting functions), UVB and UVA for both experiments. GEN(G) and GEN(T) are the generalized plant action spectrum calculated with two different formulations. FLAV is the action spectrum for the accumulation of the flavonoid mesembryanthin in *Mesembryanthemum crystallinum*, CIE is the action spectrum for UV-induced erythema in human skin and DNA(P) is the action spectrum for DNA damage in alfalfa (*Medicago sativa*) seedlings.

A. Light treatments for parental plants in the field (experimental period: early May to early June of 2016).

Light treatment	UVB (mmol m^{-2} day^{-1})	UVA (mol m^{-2} day^{-1})	GEN(G) (kJ m^{-2} day^{-1})	GEN(T) (kJ m^{-2} day^{-1})	CIE (kJ m^{-2} day^{-1})	FLAV (kJ m^{-2} day^{-1})	DNA(P) (kJ m^{-2} day^{-1})
$+UV_{parental}$	45.9	3.32	2.30	3.88	2.28	8.29	17.64
$-UV_{parental}$	0.008	2.01	0.0003	0.0008	0.17	0.005	0.56

B. Light treatments for the offspring in growth chambers.

Light treatment	UVB (mmol m^{-2} day^{-1})	UVA (mol m^{-2} day^{-1})	GEN(G) (kJ m^{-2} day^{-1})	GEN(T) (kJ m^{-2} day^{-1})	CIE (kJ m^{-2} day^{-1})	FLAV (kJ m^{-2} day^{-1})	DNA(P) (kJ m^{-2} day^{-1})
UVB+Blue+ UVB+Blue−	67.85	0.14	11.8	12.28	6.83	14.24	16.82
UVB−Blue+ UVB−Blue−	0.025	0.068	< 0.000001	0.06	0.04	0.25	0.64

1

1